8-2012

Cell Bioenergetics in Leghorn Male Hepatoma Cells and Immortalized Chicken Liver Cells in Response to 4-Hydroxynonenal Induced Oxidative Stress

Alissa Laura Piekarski
University of Arkansas, Fayetteville

CELL BIOENERGETICS IN LEGHORN MALE HEPATOMA CELLS AND IMMORTALIZED CHICKEN LIVER CELLS IN RESPONSE TO 4-HYDROXYNONENAL-INDUCED OXIDATIVE STRESS

CELL BIOENERGETICS IN LEGHORN MALE HEPATOMA CELLS AND IMMORTALIZED CHICKEN LIVER CELLS IN RESPONSE TO 4-HYDROXYNONENAL-INDUCED OXIDATIVE STRESS

A thesis submitted in partial fulfillment
of the requirements for the degree of
Master of Science in Poultry Science

By

Alissa L. Piekarski
University of Pittsburgh
Bachelor of Science in Biological Sciences, 2008

August 2012
University of Arkansas

ABSTRACT

Bioenergetic mechanisms responsible for ATP production are essential in carrying out maintenance and cell-specific functions. In this study, hepatocytes (liver cells) were used to test both endogenous and exogenous stress on cellular respiration. The secondary lipid peroxide, 4-hydroxynonenal (HNE), was used because it alters bioenergetics by increasing mitochondrial proton leak that attenuates mitochondrial radical production and, therefore, endogenous oxidative stress. The major objective of this study was to demonstrate effects of HNE-induced oxidative stress on avian hepatocyte bioenergetics. Various chemical which help enable the determination of oxygen (O_2) consumption linked to ATP synthesis (oligomycin), maximal O_2 consumption (FCCP), and proton leak (antimycin a) were used during bioenergetic analysis. Results indicated that both hepatocyte cell lines used exhibited increases in maximal O_2 consumption in response to 5 and 10 μM HNE, whereas 30 μM HNE enhanced proton leak.

This thesis is approved for recommendation to the Graduate Council.

Thesis Director:

_____
Dr. W.G. Bottje

Thesis Committee:

_____
Dr. C. Maxwell

_____
Dr. R. Wideman

_____
Dr. B.W. Kong

_____
Dr. B.M. Hargis

THESIS DUPLICATION RELEASE

I hereby authorize the University of Arkansas Libraries to duplicate this thesis when needed for research and/or scholarship.

Agreed_____
Alissa L. Piekarski

Refused_____
Alissa L. Piekarski

ACKNOWLEDGEMENTS

The author would like to express sincere thanks to Dr. W. G. Bottje for his excellent guidance, support, and friendship as an advisor throughout this Master's program. Thanks also go to K. Lassiter for his help, friendship, and wealth of knowledge as well as to B.W. Kong for use of his cell line and plethora of information about cell culture and viability.

Deepest appreciation and gratitude is extended to Dr. B.M. Hargis, Dr. B.W. Kong, Dr. R. Wideman, and Dr. C. Maxwell for serving on this thesis committee. Additional thanks go to the faculty and staff at the Poultry Science Center for kindness, support, and assistance throughout the program. A special thanks goes to C. Kremer for advice, support, and friendship; N. Mitchell for friendship, laughter, and helping to get through long nights of studying for finals and writing this thesis; and D. Welsher for undying support and believing I could accomplish anything I put my mind to.

Finally, I would like to thank my parents, brother, and family members for their prayers, support, and sacrifices made throughout the years to make this dream possible. Without you I would never have come so far and would never be able to dream this big. Any and all accomplishments I make in life are dedicated to you always; I love you all so much.

TABLE OF CONTENTS

ACKNOWLEDGEMENTS……..i.
LIST OF ABBREVIATIONS……...ii.
LIST OF TABLES……iii.
LIST OF FIGURES…….....iv.
LIST OF PAPERS…….....v.

CHAPTER 1
REVIEW OF LITERATURE…….....1
A. Overview of Bioenergetics……....1
B. Flux Analysis…….5
C.Overview of LMH cell line…….....8
D. Overview of Immortalized cells……...10
E. Overview of 4-HNE……..11
F.Seahorse Related Publications……...12
G. Objectives…….....15
H.Literature Cited…….....16

CHAPTER 2

CELL BIOENERGETICS IN LEGHORN MALE HEPATOMA CELLS AND IMMOTALIZED CHICKEN LIVER CELLS IN RESPONSE TO 4-HYDROXYNONENAL-INDUCED OXIDATIVE STRESS……..20
A. Literature Cited.....41

APPENDICIES

APPENDIX I
A. Cell Culture and Plating……62
B. Preparation of Chemicals to be Pneumatically Injected……63
C. Pyruvate Additions……64
D. Preparation and Execution Seahorse XF Analyzer……...65

APPENDIX II
A. Assessment of bioenergetics in intestinal tissue from neonatal broiler chicks…….....66
B. Literature Cited.....73

CONCLUSION.....77

LIST OF ABBREVIATIONS

AA – Antimycin A
ALDH2 – Aldehyde dehydrogenase 2
ATP – Adenosine Triphosphate
BOFA – Baseline, oligomycin, FCCP, Antimycin A
CELi-im – Chicken Embryo Liver cells-immortalized (spontaneously)
CsA – Cyclosporin A
DMEM – Dulbecco's Modified Eagle Medium
DMSO – Dimethyl sulfoxide
DNA – Deoxyribonucleic acid
ECAR – Extracellular Acidification Rate
ETC – Electron transport chain
FADH – Reduced flavin adenine □inucleotide
FCCP – carbonyl cyanide 4-trifluoromethoxyphenylhydrazone
LMH – Leghorn Male Hepatoma
NADH – Nicotinamide Adenine Dinucleotide
NADPH – Reduced □inucleotide adenine □inucleotide (phosphate)
OCR – Oxygen Consumption Rate
PBS – Phosphate buffered saline
ROS – Reactive oxygen species
TCA cycle – Tricarboxylic Acid Cycle
XF – Extracellular Flux

LIST OF TABLES

Table 1.1…….8
Table 2.1…….43
Table 2.2…….44

LIST OF FIGURES

Figure 1.1…….3
Figure 1.2…….4
Figure 1.3…….6
Figure 2.1…….45
Figure 2.2…….46
Figure 2.3…….47
Figure 2.4…….48
Figure 2.5…….49
Figure 2.6…….50
Figure 2.7…….51
Figure 2.8…….52
Figure 2.9…….53
Figure 2.10……...54
Figure 2.11……...55
Figure 2.12……...56
Figure 2.13……...57
Figure 2.14……...58
Figure 2.15……...59
Figure 2.16……...60
Figure 2.17……...61

LIST OF PAPERS

Piekarski A.L., Lassiter, K., Byrne, K., Hargis, B.M., and W.G. Bottje. 2011. Assessment of bioenergetics in intestinal tissue from neonatal broiler chicks. Abstract: Poult. Sci. 90(1):179

Piekarski A.L.*, K. Lassiter, B-W. Kong, B. M. Hargis and W. G. Bottje. 2012. Cell bioenergetics in Leghorn Male Hepatoma cells and immortalized Chicken liver cells in response to 4-Hydroxynonenal-induced oxidative stress. Poult. Sci. 91(E-supp. 1.1) #142.

Chapter 1

I.Overview of Bioenergetics:

The ability to harness energy from a variety of metabolic pathways is a property that can be found in all living organisms. Bioenergetics is a branch of science that deals with this movement of energy flow through a living system producing cellular energy mainly in the form of ATP. Over the years, advances in technology have allowed scientists to study these movements in more efficient ways. To date, quantification of oxygen consumption in cultured cells, or isolated mitochondria, has been largely performed using Clark electrodes with the cells or mitochondria suspended in stirred, buffered solution (Clark et al., 1953). This method requires that the cells be removed from their growth substrate and added to a solution that is continually stirred. Stirring may cause a result known as non laminar shear that can lead to increased oxidative stress (De Keulenaer et al., 1998).

The most current method of studying cellular bioenergetics involves monitoring changes (flux) in oxygen (O_2) and hydrogen ion (H^+) levels. Flux analysis data derived using a Seahorse Flux Analyzer, (Seahorse Biosciences, Billerica, MA) has been shown to be compared favorably to data obtained with a Clark+electrode but has the advantage of measuring flux without the need to continually stir cells or mitochondria (Dranka et al., 2011). Flux analysis measures oxygen consumption rate (OCR) and extracellular acidification rate (ECAR) from cells or mitochondria. A key to measuring OCR and ECAR is the creation of a very small (7 µl) volume of media above the cells. OCR is a measure of cellular respiration, and ECAR is a result of proton production e.g. through glycolysis. Measurements are obtained via sensors on the cover plate, that contain two fluorophores for analyte detection, one for O_2 and the other for protons. The instrument will continue to measure concentrations until the rate of change is linear and will then calculate the

slope to determine OCR and ECAR, respectively (Seahorse Biosciences). This method utilizes a cellular context within which bioenergetics of mitochondrial oxidative phosphorylation and glycolysis are examined while simultaneously reducing effects of reactive oxygen species and reactive nitrogen species on bioenergetic analysis as was previously seen in methods using the Clark electrode (e.g. Dranka et al., 2011).

By measuring oxygen and hydrogen ion flux response to a number of chemical inhibitors, it is possible to chemically 'dissect' individual components of cell bioenergetics associated with glycolysis, the Kreb cycle (or tricarboxylic acid [TCA] cycle), proton motive force, proton leak, and ATP synthesis on the electron transport chain (oxidative phosphorylation) as described below. These various components of cell bioenergetics are outlined in Figure 1.1.Glycolysis is the metabolic pathway that converts glucose into pyruvate. Free energy released from this pathway is used to form ATP and NADH. The TCA cycle, or Kreb's cycle, is used by organisms to produce energy through oxidation of carbohydrates and fatty acids into carbon dioxide and water (Lehninger et al., 1993) (Figure 1.1). The process of oxidative phosphorylation, which takes place on the inner mitochondrial membrane, is an ordered chain of events where electron transfer occurs between an electron donor and acceptor as shown in Figure 1.1. A proton motive force is generated that is used to drive ATP synthesis as protons flow back through ATP Synthase Complex V.

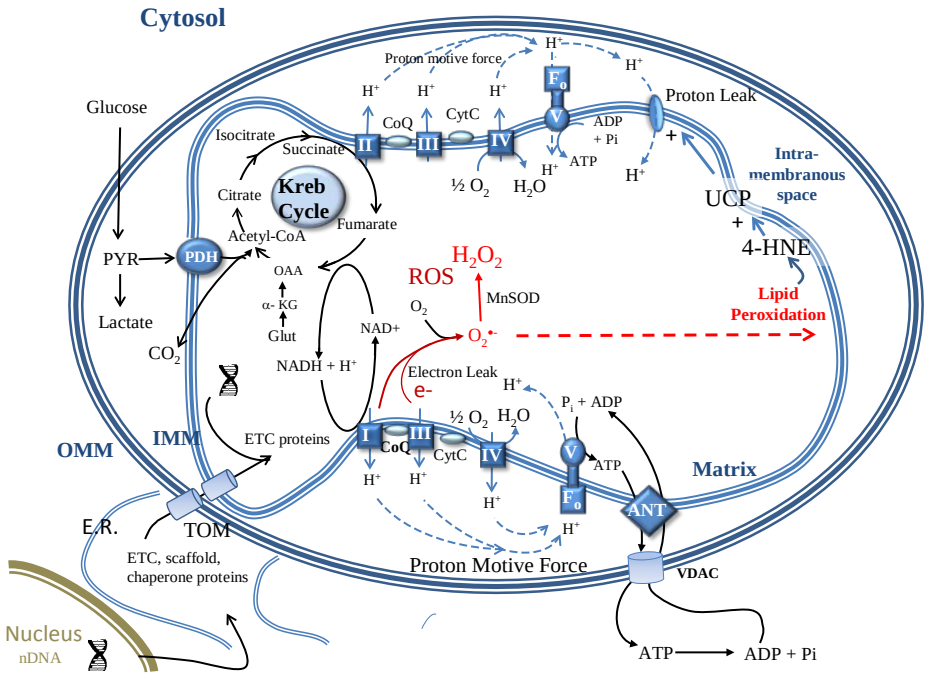

Figure 1.1: Overview of cell bioenergetics. An overview of cell bioenergetics showing energy production in the cell from glycolysis, that takes place in the cytosol, and in the mitochondria via the Kreb cycle and mitochondrial oxidative phosphorylation (Lehninger et al. ,1993). The respiratory chain consists of 5 multiprotein complexes (Complex I, II, III, IV and V) that reside on the inner mitochondrial membrane (IMM). Electrons from NADH-linked and $FADH_2$-linked substrates enter at Complex I and II respectgively and are transferred to the final electron acceptor oxygen (O_2) that is fully reduced to water. As electrons flow down the respiratory chain, protons are pumped into the intramembranous space that produces a proton motive force (dashed lines) that is used to drive ATP synthesis from ADP and Pi as protons move through the ATP synthase (Complex V). Flux analysis detects hydrogen ions produced by glycolytic activity of cells and oxygen consumption associated with mitochondrial oxidative phosphorylation (OXPHOS). Mitochondrial inefficiencies include proton leak and electron leak. Protons may move back into the mitochondrial matrix at sites other than the ATP synthase in process known as proton leak that dissipates the proton motive force without concomitant synthesis of ATP. Leakage of electrons from the respiratory chain result in the formation of superoxide ($O_2^{-\cdot}$) and several other reactive oxygen species (ROS). Oxidation of lipids by ROS can lead to lipid peroxidation and formation of a secondary lipid peroxide, 4-hydroxy 2-nonenal (4-HNE). 4-HNE has been shown to increase proton leak via increased activity of uncoupling proteins (UCP's).(Adapted from Bottje and Carstens, 2012).

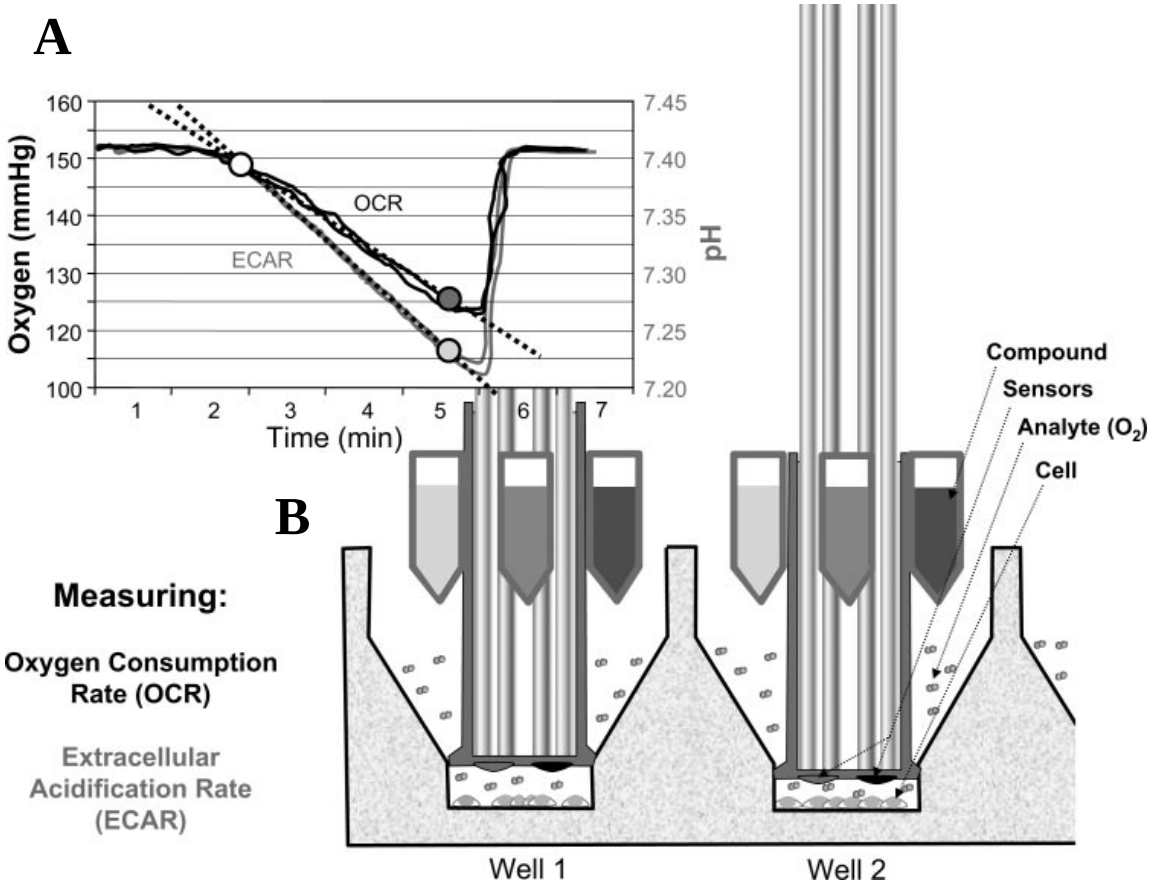

Figure 1.2: Depiction of A.) Determination of oxygen consumption rate (OCR) and extracellular acidification rate (ECAR) based on slopes of changes in oxygen and pH in the media B.) Probes containing light guides that detect levels of oxygen and hydrogen ion in the media surrounding a monolayer of cells in each well (see text for details) (Reproduced with permission from Seahorse Biosciences, Billerica MA, from Wu et al., (2007)

II. Flux Analysis:

Bioenergetics of cells can be measured using an XF24 Flux Analyzer (Seahorse Biosciences). As mentioned earlier, the XF24 Analyzer creates a transient 7 μL chamber in specialized microplates that allows OCR and ECAR to be monitored in real time. For the 24-well XF Analyzer, the kit contains a disposable sensor cartridge embedded with 24 pairs of fluorescent biosensors that are coupled to a fiber-optic waveguide (Wu et al., 2007). Light is passed through the waveguide and into optical filters to a set of highly sensitive photodetectors that are uniquely designed to measure a particular analyte (Wu et al. 2007). Each sensor cartridge also contains four ports in which different chemicals may be pneumatically injected into the media at multiple points during an experiment (Figure 1.2). Mixing of chemicals in media is carried out by the movement of the sensor cartridge and probes. These biosensors are individually calibrated at the beginning of the experiment to determine a unique sensor gain based on output measured in a reagent of known pH and oxygen concentration (Wu et al., 2007). Because XF measurements are nondestructive, other types of biological assays such as cell viability can be performed on the same cells after completion of the experiment. Prior to each experiment, the culture medium for the cell monolayer is changed to unbuffered DMEM (Dulbecco's modified Eagle's medium, pH 7.4) and placed in a non-CO_2 incubator for one hour. While the culture plate is incubating, any chemical treatments that will be used (e.g. energy substrates, inhibitors, treatments such as oxidants or antioxidants) will be added to the injection ports on the sensor cartridge. Once prepared, the cartridge is then placed into the flux analyzer for calibration of each of the O_2 and proton sensors corresponding to each well (24 pairs of sensors).

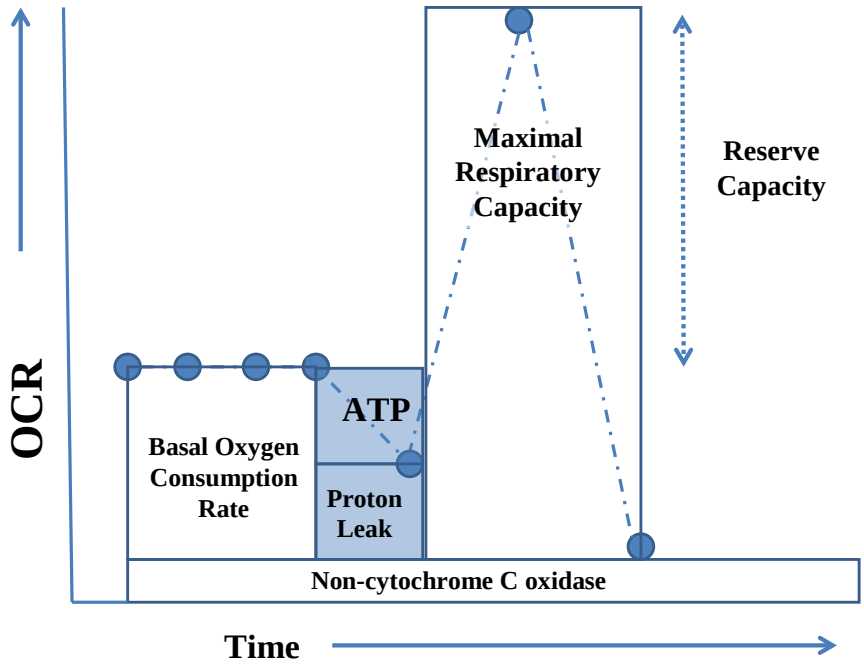

Figure 1.3: Measurement of indices of mitochondrial function using 'BOFA' analysis that is derived by measuring oxygen consumption rate (OCR) during basal conditions [B], that is followed by treatment of cells with oligomycin [O], FCCP [F], and Antimycin A [A]) (From Hill et al., 2009). The decrease in OCR following oligomycin is attributed to ATP synthesis from ATP synthase activity. The treatment of cells or mitochondria with FCCP results in a maximal respiratory capacity of the cells. By subtracting basal OCR from maximal OCR, the reserve capacity of cells can be determined. Antimycin A (a Complex III inhibitor) blocks respiratory chain activity. By subtracting antimycin A inhibited OCR from oligomycin-inhibited OCR, the amount of oxygen consumed by proton leak in the cells can be determined. The remaining OCR following treatment of cells reveals non-cytochrome C oxidase-linked OCR which is comprised primarily of non-mitochondrial oxygen consumption (e.g. cellular activities of NADPH oxidase) as well as other oxygen consuming reactions such as the formation of reactive oxygen species from leakage of electrons from the electron transport chain.

After the sensors are calibrated, the plate containing the cells and the calibrated sensor cartridge are placed in the analyzer. Components of cellular bioenergetics can be revealed by the sequential treatments of cells with various chemicals that facilitate chemical 'dissection' of bioenergetics. This chemical dissection of mitochondrial function can be carried out using a 'BOFA' analysis (e.g. Wu et al., 2007; Hill et al., 2009; 2010) that consists of establishing

measurements of: Baseline OCR, Oligomycin, FCCP (carbonyl cyanide-*p*-trifluoromethoxy-phenylhydrazone), and Antimycin A. As shown in Figure 1.3, after baseline OCR is obtained, Oligomycin, FCCP, and Antimycin A are introduced into the wells in sequence to block ATP synthase activity, uncouple the electron transport chain (to reveal maximum OCR capability), and to block electron transport at Complex III, respectively. Parameters calculated from OCR response to these chemicals represent: 1.) OCR consumption linked to ATP synthesis, 2.) OCR reserve capacity, 3.) OCR due to proton leak and 4.) non- cytochrome c oxidase OCR as shown in Table 1.1. The O_2 reserve capacity represents the maximal respiration of cells (e.g. when needed for repairing structures damaged by oxidative stress) and is calculated by subtracting basal OCR from maximal OCR (following FCCP injection). Proton leak (dissipation of proton motive force without concomitant ATP synthesis) is determined as the difference between ATP synthase OCR following oligomycin and electron inhibition by Antimycin A. Oxygen consumption following Antimycin A treatment is due to oxygen use by mechanisms other than cytochrome c oxidase; e.g. oxidases (e.g. NADPH or xanthine oxidase) or formation of mitochondrial ROS.

Carbonyl cyanide-*p*-trifluoromethoxyphenylhydrazone, (FCCP) releases the flow of electrons in the respiratory chain and increases re-oxidation of NADH into NAD^+ by complex I (Figure 1.1); thereby depleting NADH (Constantini et al., 1996; Catisti and Vercesi,1999).

Table 1.1: Equations used for calculations of mitochondrial bioenergetics based on oxygen consumption of cells in during basal respiration (Basal) and following sequential additions of oligomycin (Oligo), FCCP and antimycin A (Anti-A) as previously described (Hill et al.,. 2009; 2010; Dranka et al., 2011).

Bioenergetic Component		**Equation**
OCR linked to ATP synthesis	=	OCR_{Basal} - OCR_{Oligo}
Oxygen Reserve Capacity	=	OCR_{FCCP} - OCR_{Basal}
OCR linked to Proton Leak	=	OCR_{Oligo} - OCR_{Anti-A}
Non-cytochrome c oxidase OCR	=	OCR_{Basal} - OCR_{Anti-A}

III. Overview of LMH cell line

The first avian cell lines were produced by avian virus-induced lymphomas (Langlois et al., 1976) or leukemias (Pfeifer et al., 1980). The development of a hepatoma cell line from diethylnitrosamine-induced primary hepatocellular carcinoma in a male leghorn was performed by Kawaguchi et al (1987). These cells retain a number of phenotypic traits of chicken hepatocytes seen through chromosomal analysis (Kawaguchi, et. al., 1987) have been utilized in cancer research as well as investigation of heme biosynthesis, transfection with lipids, and propagation of some infectious poultry diseases. The biochemical and chromosomal properties of LMH cells, that includes a triploid karyotype with six marker chromosomes, remain constant over a prolonged period of propagation in culture (Kawaguchi et al., 1987). Kolluri et al. (1999) studied LMH cells to determine if they were a good model for heme biosynthesis as compared to CELCs (Chick Embryo Liver Cells) in primary cell culture. CELCs are a widely used model; however, they have some limitations that include heterogeneity, the need for weekly isolation

and establishment of primary cell cultures that introduces variation from isolation to isolation, and are also short-lived cells that limit conducting extended time course and transfection studies (Kolluri et al., 1999). Response of ALA (5-Aminolevulinic acid synthase), the rate-controlling enzyme of heme biosynthesis, was tested between the two cells lines. Kolluri et al. (1999) concluded that LMH cells are indeed a useful model for hepatic heme biosynthesis and regulation of ALA synthase. Since CELCs are not suitable for transfection studies due to their short lifespan, LMH cells are used often in transfection studies (Kolluri et al., 1999). Walzem et al. (1997) studied transfection of avian LMH-2A hepatoma cells with cationic lipids. LMH-2A is a variant of the LMH cell line and is an estrogen-responsive avian hepatoma cell line where very little is known about its susceptibility to cationic-lipid-mediated transfection.

The LMH cell line has recently been touted as a convenient culture system that responds well to phenobarbital (PB) and PB-like inducers to the same extent that primary chicken hepatocytes respond (Handschin et al., 2001). This cell line has also been used in experiments investigating mechanisms of action of leptin and its receptor in hepatocytes. Cassy et al (2003), discovered that leptin and its receptor mRNA are expressed in LMH cells, confirming previous findings of leptin expression in chicken hepatocytes (Simon et al., 1991; Taouis et al., 1993). Based on these results, Cassy et al (2003) hypothesized that leptin expression may play a key role in lipid metabolism and lipogenesis in avian species.

Being a primary hepatocellular carcinoma cell line, LMH cells are also potentially useful for comparative investigations of biological parameters such as chromosomal analysis, enzyme markers (Glucose 6-phosphatase), and tumorigenicity (Kawaguchi et al., 1987). This, along with the aforementioned studies, is why these cells were chosen to focus research on the bioenergetics of LMH cells.

III. Overview of Immortalized cell lines

Immortalized cell lines are different than the more commonly used primary cell lines. Primary cells reach senescence after a limited number of population doublings making it necessary for scientists to re-establish fresh cell cultures, a process that is time consuming and may result in variability from isolation to isolation as outlined above. On the other hand, immortalized cells such as HeLa cells (described below) can continue to grow and be passaged indefinitely as long as culture conditions are maintained, providing an inexhaustible supply of cells that can be used as models of human or animal tissues (Lonza, 2012). Because of this extended replicative capacity in immortalized cells, researchers have access to cells that exhibit the same phenotypic characteristics throughout a research project. There are several ways cells can become immortal that include: virus induction; e.g. by enhancing the expression of specific proteins or enzymes such as telomerase which plays a crucial role in cellular proliferation and tumorigenesis (Wick et al., 1999); and co-expression of specific proteins with tumor suppression genes (Biocat, 2012).

Immortalized cell lines have been used to study a multitude of biological mechanisms. Perhaps the most common example of an immortalized cell line is the HeLa line which is a cervical carcinoma transformed by human papilloma virus 18 (HPV18) (Hall et al., 2003). These cells are adherent and maintain contact inhibition, the natural process of stopping cell growth when two or more cells come into contact with each other as they grow across a culture dish. In the present study, cell bioenergetics will be investigated in an immortalized avian liver cell line developed by Lee et al (2010). Many immortalized mammalian cell lines (e.g. rat, human, porcine) have been developed and are valued for their continuous proliferation, as well as ability to express stable liver-specific functions. Such qualities are useful for in vitro toxicity

testing in the pharmaceutical, chemical, food and even cosmetics industry (Anderson et al., 1996). It has been found that an immortalized rat hepatocyte line appears to have potential for predicting toxicity of a model compound, menadione (a synthetic chemical compound used as a nutritional supplement due to its vitamin K activity), by measuring the activities of DT-diaphorase and NADPH cytochrome c reductase (Anderson et al., 1996). Immortalized human hepatocytes that are transformed with SV40 virus large T-antigen, Fa2N-4 cells, have been proposed as a tool to identify cytochrome P4503A4 (CYP3A4) inducers. CYP3A4 is the principal drug-metabolizing enzyme in the human liver and drug-drug interactions (DDIs) caused by induction of CYP3A4 can result in decreased exposure to co-administered drugs, with potential loss of efficacy (Ripp et al., 2006).

IV. Overview of 4-HNE

The α,β-unsaturated hydroxyalkenal, 4-hydroxy-2-nonenal (4-HNE), is produced during the oxidative lipid breakdown of biological membranes. It is normally found in animal tissue and in higher amounts during oxidative stress. It is known to modulate various biochemical processes in normal liver and hepatoma cells (Canuto et al., 1993), that are well recognized for their ability to withstand oxidative stress associated with the production of 4-HNE (Esterbauer et al., 1991). It is believed that the effects of 4-HNE are related to the quantity formed in the cells and the ability of the cell to metabolize or succumb to it once a critical threshold is reached. Previous studies have shown that hepatocytes can metabolize 4-HNE into its glutathione conjugate that will then be rapidly exported out of the cell to avoid reaching threshold and, ultimately, cell death (Shearn et al., 2011). With some liver cell lines, 4-HNE exposure at high concentrations (e.g. 100 μM) for two hours did not induce cell damage or death (Stewart et al.,

2009). Further studies in immortalized retinal extracts have shown that several proteins are 4-HNE-modified, (HNE adducts) and that their abundance increases with age (Kapphahn et al., 2002). These studies demonstrate that the effects of 4-HNE may differ in a primary cell line versus an immortalized cell. HNE can also be described as creating a simple feedback loop that aides in the protection of the cell.

Brand et al., (2004) showed that UCPs (uncoupling proteins) may cause mild uncoupling in response to matrix superoxide production and the release of molecules such as HNE that activate proton conductance of UCPs and other proteins. Because of the mild uncoupling, proton motive force decreases while respiration rate increases. This activity leads to a lowering of local oxygen concentration and the formation of superoxide and other reactive oxygen species (Skulachev et al., 1996). The feedback loop would act as a short-term fine control over mitochondrial ROS production by balancing the need for high proton motive force and high energy production against the need for minimal ROS production (Brand et al., 2004). This can create a self-limiting cycle to protect the cell against excessive superoxide production at the cost of a small increase in respiration and basal metabolic rate.

V. Seahorse Related Publications

Since Seahorse Biosciences (Billerica, MA) launched their product, many new insights into the biological processes of cells have been discovered or elaborated upon. Fields such as neuroscience, cardiology, and toxicology, to name a few, all have published papers using a Seahorse Flux Analyzer (Sauerbeck et al., 2012; Hill et al., 2010; Xu et al., 2011). Mitochondrial toxicity has been a serious concern, not only in preclinical drug development but also in clinical trials (Xu et al., 2011). Several distinct metabolic processes including β-

oxidation, TCA cycle, and OXPHOS, contain linked steps, owing to the importance of detection of inhibition of any one of these processes during mitochondrial toxicity models. However, detection can be complicated because intermediate endogenous metabolites can be recycled in situ or circulated systemically in other organs or tissues (Xu et al., 2011). An example of such a complication has been associated with an understanding of mechanisms related to Cyclosporin A (CsA) that is commonly used for treating autoimmune diseases and to prevent allograft rejection after organ transplantation (Luo et al., 2012). Illsinger et al. (2011) and Lemmi et al. (1990) have reported that CsA inhibits fatty acid β-oxidation in mitochondria and cause accumulation of free fatty acids or triglycerides in cells. Palmitate, a free fatty acid, can induce endoplasmic reticulum stress and apoptosis in various cells including hepatocytes. Luo et al., (2012) investigated the effect of palmitic acid on CsA induced toxicity to determine whether lipids and their interaction with CsA induce toxicity. In the aforementioned study, a Seahorse Flux Analyzer was used in which HepG2 cells were treated with CsA/palmitic acid for 24 h followed by four baseline OCR measurements (Luo et al., 2012). It was found that this CsA/palmitate combination decreased OCR and increased the accumulation of lipid droplets, and resulted in impaired cellular respiration in HepG2 cells. Their findings suggest that patients with underlying diseases (obesity, diabetes, dyslipidemia, or obesity resulting from immunosuppressive therapy) that have elevated free fatty acids could be predisposed to CsA-induced toxicity (Luo et al., 2012). Fatty acid and CsA toxicity of mitochondria can produce mitochondrial dysfunction that can be exacerbated in the presence of elevated levels of nitric oxide or by low oxygen levels (hypoxia) at the mitochondrial level.

Nitric oxide regulates several mitochondrial functions including cellular respiration and biogenesis. For example, mitochondrial biogenesis can be regulated by the soluble guanylate

cyclase pathway and nitric oxide can modulate the response to hypoxia through mitochondrial-dependent and independent pathways (Zelickson et al., 2011). Reactive oxygen species will decrease the concentration of nitric oxide available to interact with cytochrome c oxidase and participate in other reactions with reactive nitrogen species to generate secondary products that impair mitochondrial function through oxidation, nitration, and inactivation of mitochondrial proteins (Shiva et al., 2005). Studies have shown that chronic ethanol consumption causes marked bioenergetic defects in hepatocytes. These defects become more pronounced with hypoxia and are associated with decreased aerobic and anaerobic ATP production (Young et al., 2006). Zelickson et al. (2011) proposed the hypothesis that hepatocytes from chronic ethanol-fed animals will have a decreased reserve capacity and, therefore, the mitochondria will be challenged metabolically to maintain bioenergetic homeostasis under which mitochondria are more sensitive to nitric oxide. The addition of nitric oxide to hepatocytes isolated from ethanol-fed animals exhibited diminished basal and ATP-linked OCR, increased proton leak, and decreased reserve capacity, as well as increased inhibition of respiration with addition of nitric oxide under hypoxic stress (Zelickson et al., 2011). These findings demonstrated for the first time changes in mitochondrial bioenergetics with a non-invasive approach to mitochondrial biology within the intact cell that previously had only been observed in isolated mitochondria. The above studies are only a few examples of the benefits of flux analysis in mitochondrial bioenergetic studies. With the current research in a broad range of fields, flux analyses is a new leader in science, giving us a more in depth view into cellular bioenergetics and mitochondrial processes.

VI. Objectives

Investigating the bioenergetics of LMH cells and immortalized chicken liver cells can help shed knowledge on the cellular mechanisms that make these lines similar and different through comparing results as those found in Kawaguchi et al (1987) that were stated earlier. Hepatocytes play a central role in metabolism and experience both endogenous and exogenous stress. Thus, the major objectives of the present study were to first establish procedures for assessing whole cell bioenergetics in two avian hepatocyte cell lines (CELi-im and LMH) that would then be utilized to determine the effects of metabolic challenge mediated by the toxic secondary lipid peroxide, 4-HNE, on various components of avian hepatocyte bioenergetics.

Chapter 1 - Literature Cited

Anderson K., Yin L., MacDonald C., Grant M.H., 1996. Immortalized Hepatocytes as In Vitro Model Systems for Toxicity Testing: the Comparative Toxicity of Menadione in Immortalized Cells, Primary Cultures of Hepatocytes and HTC Hepatoma Cells. Toxicology. 10(6):721-727.

Biocat, 2012. http://www.biocat.com/cgibin/page/sub1.pl?sub1=cell_immortalization&main_group=cell_biology

Brand, M.D., Buckingham, J.A., Esteves, T.C., Green, K., Lambert, A.J., Miwa, S., Murphy, M.P., Pakay, J.L., Talbot, D.A., Echtay, K.S., 2004. Mitochondrial superoxide and aging: uncoupling-protein activity and superoxide production. Biochem.Soc.Symp. 71:203-213

Canuto R. A., Muzio G., Maggiora M., Poli G., Biasi F., M. Dianzani U., Ferro M., Bassi A. M., Penco S., U. Marinari M., 1993. Ability of different hepatoma cells to metabolize 4-hydroxynonenal. Cell Biochemistry and Function 11(2):79-86.

Cassy, S., M. Derouet, S. Crochet, S. Dridi, and M. Taouis, 2003. Leptin and insulin downregulate leptin receptor gene expression in chicken-derived leghorn male hepatoma cells. Poultry Science. 82:1573-1579.

Catisti R, and Vercesi A., 1999. The participation of pyridine nucleotides redox state and reactive oxygen in the fatty acid-induced permeability transition in rat liver mitochondria. FEBS Lett. 464:97-101.

Constantini P, Chernyak BV, Petronilli V, and Bernardi P., 1996. Modulation of the mitochondrial permeability transition pore by pyridine nucleotides and dithiol oxidation at two separate sites. J Biol Chem. 271:6746-6751.

De Keulenaer, Gilles, Dacid Chappell, Nobukazu Ishizaka, Robert Nerem, Wayne Alexander, and Kathy Griendling, 1998. Oscillartory and Steady Laminar Shear Stress Differently Affect Human Endothelial Redox State. Circulation Research. 82: 1094-1101.

Dranka, B.P., G.A. Benavides, A.R. Diers, S. Giordano, B.R. Zelickson, C. Reily, L. Zou, J.C. Chatham, B.G. Hill, Zhang J., Landar A., and V.M. Darley-Usmar, 2011. Assessing Bioenergetic Function in response to Oxidative Stress by Metabolic Profiling . Free Radical Biol. Med.. 51: 1622-1635.

Esterbauer H, Schaur RJ and Zollner H., 1991. Chemistry and biochemistry of 4-hydroxynonenal, malonaldehyde and related aldehydes. Free Radic Biol Med 11(1):81-128.

Hall, A., and Alexander, K., 2003. RNA Interference of Human Papillomavirus Type 18 E6 and E7 Induces Senesence in HeLa Cells. Journal of Virology. 77.10: 6066- 6069.

Hill, B.G., Dranka, B.P., Zou, L., Chatham, J.C., and V.M. Darley-Usmar, 2009. Importance of the bioenergetic reserve capacity in response to cardiomyocyte stress induced by 4-hydroxynonenal. Biochemistry Journal. 424: 99-107.

Hill Bradford, Higdon A.N., Dranka B.P. and Darley-Usmar V.M., 2010. Regulation of vascular smooth muscle cell bioenergetic function by protein glutathiolation. Biochim Biophys Acta. 1797 (2):285-295.

Kapphahn, R., Babatomiwa, G., Berg, K., Feng, X., Olsen, T., and Ferrington, D., 2005. Retinal proteins modified by 4 hydroxynonenal:Identification of molecular targets. Experimental Eye Research. 83: 165-175.

Kawaguchi T, Nomura K, Hirayama Y, Kitagawa T, 1987. Establishment and characterization of a chicken hepatoma cell line, LMH. Cancer Res. 47:4460-4464.

Kolluri, Sridevi, Kimberly Elbirt, and Herbert Bonkovsky, 1999. "Heme biosynthesis in a chicken hepatoma cell line (LMH): comparison with primary chick embryo liver cells (CELC)." Biochimica et Biophysica Acta. 1472: 658-667.

Langlois. A. J.. Ishizaki, R., Beaudreau, G. S., Kummer, J. F., Beard, J. W.. and Bolognesi, D. P., 1976. Virus-infected avian cell lines established in vitro. Cancer Res., 36: 3894-3904.

Lehninger, Albert, David Nelson, and Michael Cox, 1993. Principles of Biochemistry. Worth Publishers Inc.

Lonza, 2012. http://www.lonza.com/products-services/pharma-biotech/drug discovery/conditionally-immortalized-cells.aspx

Luo Y., Rana P., Will Y., 2012. Cyclosporine A and palmitic acid treatment synergistically induce cytotoxicity in HepG2 cells. Toxicology and Pharmacology. 261(2): 172-180.

Pfeifer, S., Kallio, A., Vaheri. A., Pettersson, R., and Oker-Blom. N., 1980. Stable bone-marrow-derived cell line producing transforming avian acute leukemia virus OKIO. Int. J. Cancer, 25: 235-242.

Qian T, Herman B, and Lemasters J, 1999. The mitochondrial permeability transition mediates both necrotic and apoptotic death of hepatocytes exposed to Br-A23187. Toxicol Appl Pharmacol. 154:117-125.

Raven, Peter, George Johnson, Johnathan Losos, and Susan Singer, 2005. Biology. 7. Columbus, OH: McGraw-Hill.

Ripp, SL, JB Mills, OA Fahmi, KA Trevena, JL Liras, TS Maurer, and SM de Morais,

2006. Use of immortalized human hepatocytes to predict the magnitude of clinical drug drug interactions caused by CYP3A4 induction. Drug Metabolism and Disposition. 34(10): 1742-1748.

Sauerbeck A., Hunter R., Bing G. and Sullivan P.G., 2012. Traumatic brain injury and trichloroethylene exposure interact and produce functional, histological, and mitochondrial deficits. Exp Neurol. 234 (1):85-94.

Seahorse Bioscience XF24 Extracellular Flux Analyzer and Prep Station Installation and Operation Manual, 2009. 1. Billerica, MA: Seahorse Bioscience. 1-158.

Shearn, Colin, Rebecca Smathers, Benjamin Stewart, Kristofer Fritz, James Galligan, Numsen Hail, and Dennis Peterson, 2011. PTEN Inhibition by 4-Hydroxynonenal Leads to Increased Akt Activation in Hepatocytes. Molecular Pharmacology Fast Forward. 33.

Shiva S., Oh J.Y., Lander A., Ulasova E., Venkatraman A., Bailey S., Darley-Usmar V., 2005. Nitroxia: the pathological consequence of dysfunction in the nitric oxide-cytochrome c oxidase signaling pathway. Free Radical Biology Med. 38:297-306.

Simon, J., B. Chevalier, M. Derouet, and B. Leclercq, 1991. Normal number and kinase activity of insulin receptors in liver of genetically fat chickens. J. Nutr. 121: 379 385.

Skulachev, V. P., 1996. Role of uncoupled and non-coupled oxidation in maintenance of safely low levels of oxygen and its one-electron reductants. Quart. Reû. Biophys. 29:169–202.

Taouis, M., M. Derouet, J.P. Caffin, A. Chavanieu, and J. Simon, 1993. Insulin receptor and insulin sensitivity in a chicken hepatoma cell line. Mol. Cell. Endocrinol. 96:113-123.

Tokuichi Kawaguchi, Kimie Nomura, Yoko Hirayama, and Tomoyuki Kitagawa, 1987 Establishment and Characterization of a Chicken Hepatocellular Carcinoma Cell Line, LMH. Cancer Research, 47:4460-4464.

Walzem, RL, MA Hickman, JB German, and RJ Hansen, 1997. Transfection of Avian LMH 2A Hepatoma Cells with Cationic Lipids. Poultry Science. 76: 882-886.

Wick M., Zubov D., Hagen G., 1999. Genomic organization and promoter characterization of the gene encoding the human telomerasereversetranscriptase (hTERT). Gene. 232(1):97-106.

Wu Min, Andy Neilson, Amy L. Swift, Rebecca Moran, James Tamagnine, Diane Parslow, Suzanne Armistead, Kristie Lemire, Jim Orrell, Jay Teich, Steve Chomicz, and David A. Ferrick, 2007. Multiparameter metabolic analysis reveals a close link between attenuated mitochondrial bioenergetic function and enhanced glycolysis dependency in human tumor cells. Am J Physiol Cell Physiol. 292: 125-136.

Young T., Bailey S., Van Horn C., Cunningham C., 2006. Chronic ethanol consumption decreases mitochondrial and glycolytic production of ATP in liver. Alcohol Alcohol. 41: 254-260.

Zelickson B., Benavides, G., Johnson M., Chacko B., Venkatraman A., Landar A., Betancourt A., Bailey S., Darley-Usmar V., 2011. Nitric oxide and hypoxia exacerbate alcohol-induced mitochondrial dysfunction in hepatocytes. Biochimica et Biophysica Acta. 1573-1582.

Chapter 2

Cell bioenergetics in Leghorn Male Hepatoma cells and immortalized Chicken liver cells in response to 4-Hydroxynonenal-induced oxidative stress[1]

*Piekarski A., *, K. Lassiter, B-W. Kong, B. M. Hargis and W. G. Bottje*

Dept. of Poultry Science, Center of Excellence for Poultry Science, University of Arkansas, Fayetteville

Correspondence to: Dr. Walter Bottje Department of Poultry Science, Center of Excellence for Poultry Science, University of Arkansas, Fayetteville, AR 72701
Tel: (479) 575-4399 FAX: (479) 575-7139
Email: wbottje@uark.edu[1]

ABSTRACT Bioenergetic mechanisms responsible for ATP production are essential in

[1] This research is published with support by the Director of the Agricultural Research Experimentation Station, University of Arkansas, Fayetteville, AR and funded in part by a grant from Arkansas Biosciences Institute (ABI) to W. Bottje.

carrying out maintenance and cell-specific functions. Hepatocytes play a central role in metabolism and experience both endogenous and exogenous stress, e.g. mitochondrial radical production and exposure to toxins. The secondary lipid peroxide, 4-hydroxynonenal (HNE), impairs protein function via HNE-adduct formation, and alters bioenergetics by increasing mitochondrial proton leak that attenuates mitochondrial radical production (and therefore endogenous oxidative stress). Thus, the major objective of this study was to demonstrate effects of HNE-induced oxidative stress on avian hepatocyte bioenergetics. After optimizing conditions (e.g. cell seeding density, chemical concentrations), mitochondrial and glycolytic activities in leghorn male hepatoma (LMH) and immortalized chicken liver (CELi-im) cells were determined by flux analysis of oxygen consumption rate (OCR) and extracellular acidification rate (ECAR), respectively, in response to 0 (Control), 5, 10, 20 and 30 μM HNE. Bioenergetic assessments were made 2 h post-HNE treatment via OCR response to oligomycin (ATP synthase inhibition), FCCP (oxidative phosphorylation uncoupler), and antimycin A (electron transport inhibition). These chemicals enable the determination of O_2 consumption linked to ATP synthesis, proton leak, and non-mitochondrial mechanisms (electron leak and oxidase activity), and maximal O_2 consumption of the cells. The results indicated that both hepatocyte cell lines exhibited increases in maximal O_2 consumption in response to 5 and 10 μM HNE whereas 30 μM HNE enhanced proton leak. This would indicate that these cells can stimulate an increase in mitochondrial energy production with low HNE levels that would enable the cells to respond to low

level oxidative stress whereas proton leak is stimulated at high HNE levels, presumably to lower mitochondrial radical production (endogenous oxidative stress) at the expense of mitochondrial function.

INTRODUCTION

Cellular energy production is fundamentally important for growth, development, and the ability of cells to respond to metabolic challenges such as oxidative stress. Mitochondria are responsible for approximately 90% of the energy production of the cell via oxidative phosphorylation, with the remainder being derived from glycolysis. Much of the understanding of mitochondrial physiology has been derived with *in vitro* studies in which cells are continuously stirred or mitochondria isolated by differential centrifugation followed by monitoring oxygen levels with a Clark-type electrode in the cell or mitochondrial suspension. A tremendous amount of knowledge of mitochondrial physiology and biochemistry has been derived from these in vitro studies, but because the method requires continual stirring of the cell or mitochondrial suspension, non-laminar shear forces can increase mitochondrial reactive oxygen species (ROS) (De Keulenauer et al, 1998; Hwang et al., 2003). Also, increased mitochondrial ROS that occurs when cells are detached from one another can cause a type of cell death termed anoikis such as that reported by Li et al. (1999). The removal of mitochondria from their normal cellular environment also cuts off communication of mitochondria with other organelles (e.g. nucleus, endoplasmic reticulum). A relatively new approach for investigating whole cell bioenergetics that does not required stirring of cells or mitochondria has been reported (Wu et. al., 2007; Ferrick et al., 2008). The flux analysis platform described in these papers monitors changes in oxygen and hydrogen ion, reflecting mitochondrial oxidative phosphorylation and glycolysis, respectively, and offers tremendous opportunities for understanding cellular bioenergetics in the context of an intact cell.

Oxidative stress occurs in cells in response to a variety of conditions ranging from disease states, toxicity, as well as during normal cellular metabolism. Oxidative damage of

membranes induces lipid peroxidation and the formation of a variety of aldehydes and peroxides including 4-hydroxy-2-nonenal (4-HNE) that is released following the peroxidation of polyunsaturated fatty acids (Esterbauer et al., 1991). The formation of 4-HNE can cause additional damage to cellular processes by forming covalent adducts with phospholipids and proteins and accentuates oxidative stress by depletion of glutathione (e.g. Benderdour et al., 2003; Yan et al., 2006). 4-HNE has now been implicated in the etiology of a number of metabolic diseases including cardiovascular disease, osteoarthritis, obesity, diabetes and metabolic syndrome (e.g. Hill et al., 2009; Mattson, 2009; Vaillancourt et al., 2008; Pillon et al., 2012). In mitochondria, a negative feedback system has been identified in which 4-HNE enhances uncoupling activities mediated by uncoupling protein and adenine nucleotide translocase that reduces superoxide production and further lipid peroxidation (Brand et al., 2004). However, the cell also must expend considerable amounts of energy to repair oxidative damage caused by 4-HNE protein adduct formation. In response to oxidative stress, cells apparently possess an ability to increase mitochondrial oxidative phosphorylation and ATP synthesis by drawing upon a bioenergetics reserve capacity (Hill et al., 2009; 2010). Irreversible loss of this reserve capacity was also demonstrated to occur during oxidative stress as well (Dranka et al., 2011).

Energy derived from cellular bioenergetics is fundamentally important for all cells to be able to grow, develop, and respond to stress such as oxidative stress. Hepatocytes in particular are very active metabolically and as such are continually undergoing endogenous oxidative stress. Whereas avian hepatocytes share many of the same metabolic characteristics to mammals, they also differ in other important areas such as fat metabolism (e.g. Leveille, 1967). To our knowledge, no studies have utilized flux analysis to study cellular bioenergetics in avian

hepatocytes or the effects of the major secondary lipid peroxide 4-HNE on avian hepatocyte bioenergetics. Thus, major objectives of the present study were to first establish procedures for assessing whole cell bioenergetics in two avian hepatocyte cell lines that would then be utilized to determine the effects of metabolic challenge mediated by the toxic secondary lipid peroxide, 4-HNE, on various components of avian hepatocyte bioenergetics. The two avian cell lines investigated in this study were the commercially available avian hepatocyte line, the male leghorn hepatoma, (LMH) cell line established by Tomoyuki Kitagawa in Tokyo, Japan (http://www.cell-lines-service.de/content/index_eng.html) and a recently established immortalized chicken embryo liver cell (CELi-im) (Lee et al., 2010).

MATERIALS AND METHODS

Chemicals and Reagents.

Reagents Oligomycin, Carbonyl cyanide-p-trifluoromethoxyphenylhydrazone (FCCP), and Antimycin A were obtained from Sigma-Aldrich, St. Louis, MO. Materials and reagents for all XF assays were provided from Seahorse Biosciences (Billerica, MA). Cell growth medis (Waymouths and DMEM) as well as 0.25% trypsin were obtained from Invitrogen-GIBCO, (Grand Island, NY), 0.4% trypan blue from VWR (Radnor, NY), and polystyrene tissue cultures dishes were from BD Falcon Biosciences (Franklin, NJ).

Growth media. LMH cells were grown in Waymouth's media containing 10% FBS, 1% PenStrep, and 1% Glutamine (Invitogen-GIBCO) , and CELi-im cells were grown in DMEM containing 10% FBS, 1% PenStrep, and 1% Glutamine (Invitrogen-GIBCO). The cells were detached from the plate using .25% 1x trypsin-EDTA (Invitrogen-GIBCO),

Assay media. Seahorse biosciences unbuffered Assay media was obtained from Seahorse Biosciences, (Billerica, MA) and contains no added glucose, sodium pyruvate, or Glutamax (Seahorse Bioscience Manual).

Cell lines and Viability.

The LMH cells were obtained from a commercial source, ATCC (CRL-2117) (www.atcc.org) whereas the CELi-im cells were developed by Kong and co-workers (Lee et al., 2010). Cells were frozen in cryo-tubes in liquid nitrogen and, prior to use, were thawed out and plated in 100 x 20 mm polystyrene tissue culture dishes. After about 2 to 4 days (one to three passages) sufficient growth was observed in both the CELi-im and LMH cells. The cells were then detached from the tissue culture plate using 0.25% 1x trypsin-EDTA (Invitrogen-GIBCO),

gently centrifuged at 1000 rpm for 5 min, and resuspended in 1 to 2 mL of media. The numbers of viable cells were determined by trypan blue exclusion using trypan blue (0.4% in NaCl). Viable cells were counted using a hemocytometer and the percent of live cells were determined using the equation:

Total cells alive/total cells dead and alive = percent alive

After calculating the number of viable cells, 100 µL of media containing a known quantity of CELi-im and LMH cells was added to each well. One hundred µL of growth media alone was added to each of the four background correction wells. After 1 h of incubation (37°C, 5% CO_2) to allow cells to settle, an additional150 µL of growth media was carefully added and the plates placed in a CO_2 incubator overnight (18 to 20 h) to allow cells to attach and form a nearly confluent monolayer in the wells. The following day, the cells were washed in 1 mL unbuffered Seahorse assay media (2.25 g Glucose in 500 mL XF Assay media, pH 7.4) followed by the addition of 575 µL of media in each well. The plate was then placed into a non-CO_2 incubator for 1 h prior to start of an experiment. During this time, the sensor cartridge was calibrated using a software program (Seahorse Biosciences, Billerica, MA) described in the operation manual. After the 1 h incubation period, the 24 well plate and sensor cartridge were placed in the XF24 flux analyzer. Optimal seeding densities (based on OCR and ECAR assessment over 1 to 2 h) were 100,000 and 50,000 cells per well for CELi-im and LMH cells, respectively.

Preparation of chemicals.

Chemicals used to conduct the analysis of cell bioenergetics were oligomycin, FCCP, and Antimycin A. The sequence of chemical treatments of oligomycin, FCCP, and antimycin A that is preceded by measurement of basal respiration is termed 'BOFA' analysis (Hill et al., 2009; 2010; Dranka et al., 2011). All chemicals were kept frozen at 4°C and thawed out for use the day of experiment. Concentrations of chemicals were prepared as follows: Oligomycin was diluted with DMSO from a stock concentration of 50 mM to a working concentration of 1 mM; FCCP was diluted in DMSO from stock solution of 30 mM to a working concentration of 300 µM; and antimycin A was diluted with DMSO to a working concentration of 1 mM. The secondary lipid peroxide, 4-HNE, was diluted using ethanol from a stock concentration of 64 mM to the desired concentration range (10 to 100 µM) used in experiments described below. The final 4-HNE dilution was made immediately (within 1 h) before use due to its relative instability at room temperature. Based on optimization studies, the chemical concentrations subsequent bioenergetic studies were 1 µg/mL for oligomycin and 150 to 200 nM for FCCP. Optimization of antimycin A is not required and was used at a 10 µM concentration. Final dilutions of the chemicals were made with Seahorse running media and placed into one of four injection ports for each well. After placement, the chemicals remain in the ports until they are pneumatically injected into the media in each well.

General Procedure – Flux Analysis.

An XF24 Flux Analyzer, (Seahorse Biosciences Billerica, MA) was used to conduct bioenergetic studies in CELi-im and LMH cells. The flux analyzer measures the rate of change of dissolved oxygen surrounding an adherent monolayer of cells. It does this by using a sensor cartridge embedded with 24 optical fluorescent probes that contain oxygen and pH specific

sensors. This sensor cartridge is placed inside of a calibration plate that contains 1000 μL/well of calibration buffer overnight in a 37°C non-CO_2 incubator. Prior to each experiment, the probes of the sensor cartridge are programmed to mix the assay media (by up and down movement of the probes) in each well for 3 min to allow the oxygen partial pressure (PO_2) to reach equilibrium, followed by a 2 min quiescent and 3 min measuring/data acquisition periods. Measurement is performed when the probes are lowered into the wells to form a 7 μL transient microchamber, is obtained, and flux determined, from the slopes of changes in PO_2 and hydrogen ion levels over time. Sensor cartridges, microplates, calibrant solution, and unbuffered running media (pH 7.4) were all obtained from Seahorse Bioscience. Analysis performed on cells measured OCR, ECAR, O_2, and pH either by point by point analysis or a grouped version. After obtaining OCR and ECAR during basal conditions, the cells were treated in sequence with oligomycin (1μg/mL), FCCP (150 or 200 nM final concentration), and antimycin A (10 μM).

Bioenergetic assessment was made by treating cells with Oligomycin, FCCP, and Antimycin A as previously described (Wu et al., 2007; Hill et al., 2009; 2010). Figure 2.2 illustrates how these chemicals are used in a bioenergetics analysis (i.e. BOFA analysis that refers to Basal, Oligomycin, FCCP and Antimycin A). The results of these chemical optimization studies on OCR response revealed that 1 μg/mL (1.3 μM) oligomycin and 150 to 200 nM FCCP would be optimal doses for conducting mitochondrial studies. Using OCR data obtained from this sequence of treatments enables the following to be determined; oxygen consumption associated with ATP synthesis, oxygen consumption related to maximal reserve capacity, oxygen consumption related to proton leak, and non-mitochondrial oxygen consumption. Equations used for calculations are shown in Table 2.1. Percentages of each of

the components of mitochondrial bioenergetics can be calculated using maximal respiration rate after FCCP as 100%.

Effects of 4-HNE on bioenergetics in CELi-im and LMH hepatocytes.

The effects of the secondary lipid-peroxide 4-HNE on time course changes in OCR and ECAR were determined in CELi-im and LMH hepatocytes. CELi-im cells (100,000/well) and LMH (50,000/well) were added to plates and allowed to adhere overnight. After changing the media and placing the plates in the non-CO_2 incubator, 4-HNE was added to the injection ports of the sensor plate to provide a final concentration of 10, 20, and 30 µM in the media. The control (0 µM 4-HNE) contained media with or without ethanol vehicle. After establishing basal respiration, 4-HNE was added and changes in OCR and ECAR monitored over a 4 to 5 hour period. Because little effect of 4-HNE on OCR was observed in LMH cells, a second time course study was conducted using 20 to 75 µM 4-HNE.

The effects of 4-HNE on CELi-im and LMH hepatocyte bioenergetics were determined by the sequential addition of oligomycin, FCCP, and antimycin A at 60 min post 4-HNE treatment in CELi-im cells and at 60 and 120 min post 4-HNE treatment in LMH cells. In these studies, basal respiration of cells was assessed before and after treating cells with 4-HNE. Bioenergetic assessments were made starting at 60 min post-4-HNE treatment in CELi-im and 120 min post 4-HNE treatment in LMH cells. Components of mitochondrial bioenergetics, i.e. oxygen consumption associated with ATP synthase activity, reserve capacity, proton leak, and non-cytochrome C oxidase were calculated as shown in Table 2.1.

Statistical analysis.

Values in graphs and tables represent the mean $\pm$ SE. Differences of mean values were determined by two-tailed Student's T-test (or analysis of variance) with a P value of ≤ 0.05 being considered statistically significant.

RESULTS

Optimization of conditions in CELi-im hepatocytes.

Before flux analysis studies can be conducted for a particular cell type, it is necessary to optimize conditions that include cell seeding density and concentrations oligomycin and FCCP to be used. Oxygen consumption rate (OCR, pmoles/min) in CELi-im over 180 min is shown in Figure 2.4 A and B. It can be seen that there was a clear 'dose response' effect on OCR rates and that OCR was constant in CELi-im cells with seeding densities of 50 to 200K per well (Figure 2.4A). The relationship of OCR to ECAR shown in Figure 2.4 B suggests that any of these seeding densities would be acceptable for subsequent bioenergetics studies. The 100K cell per well seeding density was chosen for subsequent studies.

Assessment of mitochondrial bioenergetics in cells requires the sequential addition of oligomycin, FCCP and antimycin A as shown in Figure 2.3. It is not necessary to optimize antimycin A levels as this is the final chemical for BOFA analysis (Hill et al., 2009; 2010; Dranka et al., 2011). The effects of different levels of oligomycin and FCCP on OCR and ECAR of CELi-im cells are shown in Figure 2.5. A maximal decrease in OCR concomitant with an increase in ECAR was observed following treatment of cells with 1 □g/mL oligomycin (Figure 2.7A, and B). The increase in ECAR that is observed is likely a compensatory response of cells to increase energy production via glycolysis as ATP synthesis is inhibited. A maximal increase in both OCR (Figure 2.5 A, and B) and ECAR (Figure 2.5C, and D) in CELi-im cells was observed in response to 150 nM FCCP. Presumably, the increase in ECAR occurred because FCCP-mediated uncoupling would not be associated with mitochondrial ATP synthesis.

Bioenergetic determination in CELi-im hepatocytes.

Bioenergetic assessment of CELi-im hepatocytes under basal conditions (unchallenged) was conducted using a seeding density of 100,000 cells/well. Changes in OCR for in response to sequential additions of oligomycin, FCCP, and antimycin A are shown in Figure 2.6. Using data in Figure 2.6 and the equation shown in Table 2.1, components of mitochondrial bioenergetics of oxygen consumption related to ATP synthesis, reserve capacity, proton leak, and non-mitochondrial cytochrome c oxidase activity were determined and presented in Table 2.2.

Effect of 4-HNE on cell bioenergetics in CELi-im hepatocytes.

The effects of 4-HNE on time course changes in OCR and ECAR in CELi-im cells are shown in Figure 2.7. After 3 basal measurements were obtained, cells were treated with either media alone, media containing ethanol vehicle, and 5 to 30 μM 4-HNE. OCR declined in control treated cells for approximately 50 min post-injection but remained constant during the remainder of the experiment. A dose response effect of 4-HNE on OCR was detected that produced declines in OCR that occurred earlier as the levels of 4-HNE increased (Figure 2.7 A). It is apparent that the ability of CELi-im cells to remain energetically functional had been severely compromised by the 30 μM 4-HNE level as indicated by the decline in OCR to almost undetectable levels. Although considerable variability in ECAR was observed in CELi-im cells following 4-HNE treatment, a dose response of 4-HNE on mean ECAR values was also observed (Figure 2.7B).

Based on the OCR response to 30 μM HNE, it was decided that the bioenergetic analysis of 4-HNE- treated cells would be initiated at 80 min (60 min post 4-HNE treatment) that corresponded to a transient rise in OCR in the 30 μM 4-HNE treated cells (Figure 2.7A). Changes in OCR and ECAR in response to 4-HNE and sequential treatments of oligomycin,

FCCP, and antimycin A are shown in Figure 2.8. Using this data and equations in Table 2.1, the effect of 4-HNE treatments on mitochondrial bioenergetics in CELi-im are shown in Figure 2.9. An inverse relationship between 4-HNE and OCR attributed to ATP synthase activity (i.e. oligomycin sensitive OCR) was observed (Figure 2.9A). Oxygen reserve capacity (that available to cells in response to a metabolic challenge) was elevated by 5, 10, and 20 μM 4-HNE compared to controls (0 μM 4-HNE) (Figure 2.9B). Proton leak was elevated at 30 μM 4-HNE but there were no differences in proton leak between 0 to 20 μM 4-HNE treatments (Figure 2.9 C). Non-cytochrome c oxidase-related oxygen consumption was higher at all levels of 4-HNE compared to controls (Figure 2.9 D).

Optimization of conditions for LMH hepatocytes.

The relationship between OCR and ECAR in LMH cells indicates that seeding densities above 50,000 cell/well caused a shift towards. increased glycolytic activity (Figure 2.10). It was also noted when LMH cells were seeded at 100,000 cells/well or greater, clumping of cells (overgrowth) was observed in the wells. This produced 'noisy' data that was deemed unusable because of the analyzers requirement that cells must form a uniform monolayer in the wells for accurate measurements to be obtained. Based on these findings, a seeding density of 50,000 cells/well was used in subsequent studies.

Bioenergetics of LMH cells.

Optimization studies were conducted and revealed similar results to those obtained with CELi-im cells (data not shown). Changes in OCR during basal respiration and in response to oligomycin (1 μg/mL; 1.3 μM) and 150 nM FCCP in LMH cells are shown in Figure 2.11 and qualitatively similar to that obtained in CELi-im cells (Figure 2.6). Oxygen consumption

associated with ATP synthase activity, reserve capacity, proton leak, and non-mitochondrial cytochrome c oxidase were calculated using equations in Table 2.1 and presented in Table 2.2.

Effect of 4-HNE on bioenergetics of LMH cells.

The effects of 4-HNE (0, 5, 10, 20 and 30 μM) on OCR and ECAR of LMH cells are shown in Figure 2.12A and B, respectively. As 4-HNE (5 to 30 μM) had little effect on OCR and ECAR, an additional study was conducted with 20 to 100 μM 4-HNE (Figure 2.13) which showed a clear compromise of LMH respiration at the 75 and 100 μM levels.

From these two experiments, it was decided that bioenergetic analysis in LMH cells would be conducted with 20 to 50 μM HNE levels and at two times (at 80 and 140 min or 60 and 120 after 4-HNE treatment). The results of these studies are shown in Figure 2.14. Using OCR data shown in Figure 2.14 A and B, the effects of 4-HNE on components of mitochondrial bioenergetics were calculated and are presented in Figure 2.15 (60 min post 4-HNE) and Figure 2.16 (120 min post 4-HNE). As in CELi-im cells, increasing levels of 4-HNE reduced oxygen consumption in LMH cells associated with ATP synthase activity at 60 min post 4-HNE (Figure 2.15A), but unlike CELi-im cells, 4-HNE had no effect on oxygen reserve capacity (Figure 2.15B), proton leak was (Figure 2.15C), or non-cytochrome C oxidase linked oxygen consumption (Figure 2.15D). At 120 min post HNE, oxygen consumption linked to ATP synthase activity, reserve capacity and non cytochrome c oxidase activity all decreased with increasing 4-HNE levels whereas oxygen consumption linked to proton leak increased in response to higher levels of 4-HNE (Figure 2.16).

DISCUSSION

One of the goals of this study was to establish procedures to assess cell bioenergetics by monitoring changes of PO_2 and hydrogen ion; i.e. flux analysis (Wu et al., 2007; Ferrick et al., 2008). Monitoring OCR during a basal state, followed by sequential treatments of cells with oligomycin, FCCP, and antimycin A enables a chemical 'dissection' of mitochondrial bioenergetics that reveals oxygen consumption associated with ATP synthase activity, proton leak, oxygen reserve capacity, and non-cytochrome c oxidase activity to be determined (Hill et al., 2009; 2010; Dranka et al., 2011.) Values for these components of mitochondrial bioenergetics for CELi-im and LMH avian hepatocytes are shown in Table 2.2 Basal OCR was considerably greater in LMH cells compared to CELi-im cells even though the seeding density for LMH cells (50K per well) was half of that used for CELi-im cells (100K/well). This likely reflects the characteristic fast growth of LMH hepatocytes. Although this precludes comparison of actual OCR and ECAR values between the 2 cell lines, comparisons can be facilitated by expressing the results as a percent of maximal OCR as shown in Figure 2.17. From these data it appears that with basal conditions (i.e. no metabolic challenge and no other energy substrates besides 25 mM glucose and 1.8 mM glutamine in the assay media), LMH cells had higher OCR related to ATP synthase activity but had lower reserve capacity and higher OCR attributed to proton leak compared to the CELi-im cells. There were no differences in OCR due to non-cytochrome c oxidase activity between the two cell lines (Figure 2.17). Each of these components of bioenergetics will be discussed in greater detail below within the context of the metabolic challenge of 4-HNE.

The secondary lipid peroxide, 4-HNE, has important electrophilic properties and reacts with proteins, lipids and nucleotides to form 4-HNE adducts (Pillon et al., 2012). Mitochondrial

proteins are particularly prone to HNE adduct formation as the mitochondria are a major source of endogenous ROS production in the cell (Echtay et al., 2003). Mitochondrial ROS production is associated with uncoupling of the mitochondrial membrane and lowering of mitochondrial membrane potential (Skulachev, 1996, Papa and Skulachev, 1997). It was subsequently demonstrated this uncoupling was the result of 4-HNE-induced dissipation of proton motive force by facilitating movement of protons (proton leak) across the mitochondrial membrane by increased activity and expression of uncoupling protein, adenine nucleotide translocase as well as glutamate and aspartate transporters (Ectay et al., 2003; Brand et al., 2004). Thus, increased 4-HNE levels in the inner mitochondrial membrane following lipid peroxidation exerts an important mechanism of attenuating endogenous oxidative stress by increasing proton translocation and lowering mitochondrial membrane potential (Brand et al., 2004). In the present study, 4-HNE treatment increased oxygen consumption attributed to proton leak in both the CELi-im and LMH cells. It appears that the CELi-im cells may be more responsive to 4-HNE compared to LMH cells which would suggest that there could be differences in the amount or activity of the various proton translocating proteins or other components of the inner mitochondrial membrane between these 2 cell lines.

Oxygen consumption associated with ATP synthase activity (mitochondrial oxidative phosphorylation) was diminished in both CELi-im and LMH cells in response to increasing levels of 4-HNE treatment. This could be due to direct damage and reduced functionality from 4-HNE protein-adducts of proteins associated with the electron transport chain (Complexes I to IV) and of ATP synthase (Complex V) as well as indirect effects due to increased oxidative stress through depletion of mitochondrial and cytosolic glutathione (Pillon et al., 2012).

It was hypothesized that an increase in oxygen consumption associated with the cellular reserve capacity following 4-HNE represents a response to a metabolic challenge of increased demand for ATP to repair oxidative damage of critical cellular structures such as proteins, nucleotides, and lipids (Hill et al., 2009; Dranka et al., 2011). In this regard, it would appear that the CELi-im cells may have greater capacity to increase energy production than do LMH cells since reserve capacity in these cells was elevated in CELi-im cells by 5 to 20 μM 4-HNE whereas a similar increase was not observed in LMH cells at the 20 μM 4-HNE treatment.

When the reserve capacity of mitochondria is depleted, cellular injury occurs as well as decreased efficiency due to proton leak and increased protein-HNE adduct formation (Hill et al., 2009). 4-HNE increases proton leak thereby decreasing mitochondrial efficiency, and represents a metabolic challenge by increasing the need for ATP to facilitate repair of damaged cellular structures (Hill et al., 2009). Proton leak across the mitochondrial inner membrane accounts for 20-30% of the standard metabolic rate in animals and represents a significant inefficiency due to energy released during substrate oxidation that is not conserved as ATP (Brand et al., 1994). Mitochondrial respiration under nonphosphorylating (state 4, resting respiration) conditions is primarily the result of leakage of protons across the mitochondrial inner membrane and may account for ~ 50% of oxygen consumption during state 4 respiration (Barger, et al., 2003).

Cytochrome c oxidase is the terminal electron acceptor in the mitochondrial respiratory chain and catalyzes the complete reduction of oxygen to water. As such, non-cytochrome c oxidase related OCR would be comprised of oxygen consuming reactions not attributed to its activity such as formation of reactive oxygen species associated with electron leak and other biochemical reactions (e.g. NADPH oxidase, cytochrome P450). In CELi-im cells non-cytochrome c oxidase related OCR was elevated in response to 4-HNE at all levels that were

tested (5 to 30 μM) (Figure 2.9D). In contrast, 40 and 50 μM 4-HNE at both 60 and 120 min post 4-HNE treatment lowered non cytochrome c oxidase activities in LMH cells (Figure 2.15D, Figure 2.16D). Since part of the non-cytochrome c oxidase oxygen consumption would be due to mitochondrial ROS production, it could be speculated that increased proton leak in the LMH cells may decrease mitochondrial ROS in LMH cells. In contrast, CELi-im cells exhibited an increase in non-cytochrome c oxidase activity with higher levels of 4-HNE treatment (Figure 2.9D) despite an increase in proton leak in response to 30 μM 4-HNE (Figure 2.9C). Further investigation would need to be conducted to determine if there are differences in activity or expression of UCP and ANT, or in lipid content that exist in the mitochondria of LMH and CELi-im cells.

In summary, procedures for assessing cellular bioenergetics in two avian hepatocyte cell lines were established. Under basal conditions, components of mitochondrial bioenergetics were determined by monitoring oxygen consumption of cells in response to sequential treatments of cells with oligomycin, FCCP and antimycin-A. These results suggest that LMH cells may have greater oxygen consumption related to ATP synthase activity and proton leak than in the CELi-im cell line whereas the CELi-im cells may possess inherently greater reserve capacity for ATP synthesis that could be called upon in response to a metabolic challenge. In response to increasing levels of 4-HNE, a secondary lipid peroxide that is formed in cells during oxidative stress, the CELi-im cells appear to be able to exhibit a greater capacity to increase ATP synthesis by drawing upon a reserve capacity that was not observed in the LMH cells. The CELi-im cells did exhibit an increase in non-cytochrome c oxidase related oxygen consumption that was not observed in the LMH cells. Further investigation of cell bioenergetics combined with gene

and/or protein expression analysis will be required to determine exact mechanisms contributing to differences in cell bioenergetics between CELi-im and LMH avian hepatocyte cell lines.

ACKNOWLEDGEMENTS

This research is published with support by the Director of the Agricultural Research Experimentation Station, University of Arkansas, Fayetteville, AR and funded in part by a grant from Arkansas Biosciences Institute (ABI) to W. Bottje.

LITERATURE CITED

ATCC, 2012. http://www.atcc.org/ATCCAdvancedCatalogSearch/ProductDetails/Tabid/452/Default.asx?ATCCNum=CRL-2117&Template=cellBiology.

Barger, J.L., Brand, M.D., Barnes, B.M., Boyer, B.B., 2003. Tissue-Specific Depression of Mitochondrial Proton Leak and Substrate Oxidation in Hiberanting Artic Ground Squirrels. American Journal of Physiology. 284(5):306-313.

Benderdour, M., Charron, G., Deblois, D., Comte, B., and Des, R. C., 2003. Cardiac Mitochondrial $NADP^+$ -isocitrate dehydrogenase is inactivated through 4-hydroxynonenal adduct formation: an event that precedes hypertrophy development. J. Biol. Chem. 278: 45154-45159.

Brand, M.D., Chien, L.F., Ainscow, E.K.., Rolfe, D.F.S., Porter, R.K., 1994. The causes and Functions of Mitochondrial Proton Leak. Biochim Biophys Acta. 1187:132-139.

Cell lines services, 2012. http://www.cell-linesservice.de/content/search_eng.html?searchform=1&raw=LMH&x=0&y=0.

Echtay, K.S., Esteves, T.C., Pakay, J.L., Jekabsons, M.B., Lambert, A.J., Portero-Otin, M., Pamplona, R., Vidal-Puig, A.J., Wang, S, Roebuck, S.J., and Brand, M.D., 2003. A signaling role for 4-hydroxy-2-nonenal in regulation of mitochondrial uncoupling. EMBO J. 22:4103-4110.

Endo, J., Sano, M., Katayama, T., Hishiki, T., Shinmura, K., Morizane, S., Matsuhashi, T., Katsumata, Y., Zhang, Y., Ito, H., Nagahata, Y., Marchitti, S., Nishimaki, K., Wolf, A.M., Nakanishi, H., Hattori, F., Vasiliou, V., Adachi, T., Ohsawa, I., Tagushi, R., Hirabayashi, Y., Ohta, S., Suematsu, M., Ogawa, S., Fukuda, K., 2009. Metabolic remodeling induced by mitochondrial aldehyde stress stimulates tolerance to oxidative stress in the ehart. Circ. Res. 105: 1118-1127.

Esterbauer H, Schaur RJ and Zollner H., 1991. Chemistry and biochemistry of 4-hydroxynonenal, malonaldehyde and related aldehydes. Free Radic Biol Med 11(1):81-128.

Higdon, Ashlee N., Benavidas, G. A., Chacko, B. K., Ouyang, X., Johnson, M. S., Landar, A., Zhang, J., Darley-Usmar, V.M., 2011. Hemin causes Mitochondrial Dysfunction in Endothelial cells Through Promoting Lipid Peroxidation: The Protective Role of Autophagy. AJP 10(1152):1-39.

Hill, Bradford, and Brian Dranka, 2009. Importance of the bioenergetic reserve capacity in response to cardiomyocyte stress induced by 4-hydroxynonenal. Biochemistry Journal. 424:99-107.

Hwang, J., A. Saha, Y. C. Boo, G.P. Sorescu, J. S. McNally, S. M. Holland, S. Dikalov, D. P. Giddens, K. K. Griendling, D. G. Harrison, and H. Jo. 2003. Oscillatory shear stress stimulates endothelial production of superoxide from $p47^{phox}$-dependent NAD(P)H oxidases, leading to monocyte adhesion. J. Biol. Chem. 278: 47291-47298.

Lee JY, and Kong BW., 2010. Continuously growing chicken liver cell lines for the vaccine production against poultry viruses. Poultry Sci 89 (E-Suppl 1): 31.

Li, A.E., I. Ito, I. I. Rovira, K-S. Kim, K. Takeda, Z-Y. Yu, V. J. Ferrans, and T. Finkel. 1999. A role for reactive oxygen species in endothelial cell anoikis. Circ. Res.85:304-310.

Papa, S., and Skulachev, V.P., 1997. Reactive Oxygen Species, Mitochondria, Apoptosis, and Aging. Mol. Cell Biochem. 174:305-319.

Pillon, Nicolas J., Croze, M.L., Vella, R.E., Laurent, S., Lagarde, M., and Soulage, C.O., 2012. The Lipid Peroxidation By-Product 4-Hydroxy-2-nonenal (4-HNE) Induces Insulin Resistance in Skeletal Muscle though Both Carbonyl and Oxidative Stress. J. Endocrinology. 153(4): 1-13.

Ryan, M. J., G.Johnson, J. Kirk, S. M. Fuerstenberg, R.A. Zager, and B. Torok-Storb, 1994. HK-2: An immortalized proximal tubule epithelial cell line from normal adult human kidney. *Kid. Inter.*. 45: 48-57.

Seahorse Bioscience XF24 Extracellular Flux Analyzer and Prep Station Installation and Operation Manual, 2009. Billerica, MA: Seahorse Bioscience, 1-158.

Shay, Jerry W., Woodring E. Wright, and Harold Werbin, 1991. Defining the molecular mechanisms of human cell immortalization. *Biochimica et Biophysica Acta*. 1072: 1-7.

Tjalkens, R. B., Lanz W. Cook, Dennis R. Peterson, 1999. Formation and Export of the Glutathioone Conjugate of 4-Hydroxy-2,3-E-nonenal (4-HNE) in Hepatoma Cells. Archives of Biochemistry andBiophysics. 361(1): 113-119.

Woodworth, C.D., and H.C. Isom, 1987. Regulation of albumin gene expression in a series of rat hepatocyte cell lines immortalized by simian virus 40 and maintained in chemically defined medium. *Mol. Cell Biology*. 7(10): 3740-3748.

Wu Min, Andy Neilson, Amy L. Swift, Rebecca Moran, James Tamagnine, Diane Parslow, Suzanne Armistead, Kristie Lemire, Jim Orrell, Jay Teich, Steve Chomicz, and David A. Ferrick, 2007. Multiparameter metabolic analysis reveals a close link between attenuated mitochondrial bioenergetic function and enhanced glycolysis dependancy in human tumor cells. Am J Physiol Cell Physiol. 292: 125-136.

Yan, J., Hales, B.F., 2006. Depletion of Glutathione Induces 4-Hydroxynonenal protein adducts and Hydroxyurea Teratogenicity in the Organogenesis Stage Mouse Embryo. JPET. 319(2):613-621.

Table 2.1: Equations used for calculations of mitochondrial bioenergetics based on oxygen consumption of cells in during basal respiration (Basal) and following sequential additions of oligomycin (Oligo), FCCP and antimycin A (Anti-A) as previously described (Hill et al.,. 2009; 2010; Dranka et al., 2011).

Bioenergetic Component		**Equation**
OCR linked to ATP synthesis	=	OCR_{Basal} - OCR_{Oligo}
Oxygen Reserve Capacity	=	OCR_{FCCP} - OCR_{Basal}
OCR linked to Proton Leak	=	OCR_{Oligo} - OCR_{Anti-A}
Non-mitochondrial OCR	=	OCR_{Basal} - OCR_{Anti-A}

Table 2.2: Components of mitochondrial bioenergetics in immortalized Chicken Embryo Liver (CELi-im) and Leghorn Male Hepatoma (LMH) hepatocytes. The values were obtained from oxygen consumption rates (OCR) data presented in Figure 2.9 and 2.12 in CELi-im hepatocytes (50,000 cells per well) and LMH hepatocytes (100,000 cells per well), respectively,

Bioenergetic Component	Equation	CELi-im[1] OCR (pmol/min)	LMH[1] OCR (pmol/min)
OCR linked to ATP synthesis	OCR_{Basal} - OCR_{Oligo}	137.5 ± 7.1	`310.7 ± 13.1
Oxygen Reserve Capacity	OCR_{FCCP} - OCR_{Basal}	93.4 ± 9.9	123.7 ± 11.6
OCR linked to Proton Leak	OCR_{Oligo} - OCR_{Anti-A}	31.7 ± 1.2	85.7 ± 2.6
Non-mitochondrial cytochrome c oxidase OCR	OCR_{Basal} - OCR_{Anti-A}	54.0 ± 4.5	115.3 ± 5.4

[1] Values represent the mean ± SE (n=20)

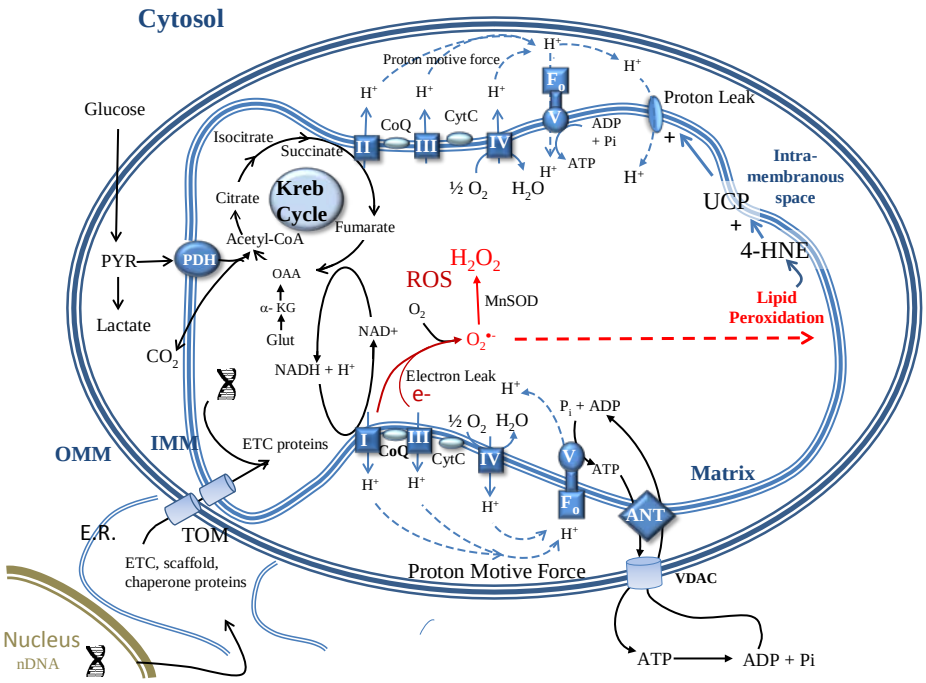

Figure 2.1: Overview of cell bioenergetics. An overview of cell bioenergetics showing energy production in the cell from glycolysis, that takes place in the cytosol, and in the mitochondria via the Kreb cycle and mitochondrial oxidative phosphorylation (Lehninger et al. ,1993). The respiratory chain consists of 5 multiprotein complexes (Complex I, II, III, IV and V) that reside on the inner mitochondrial membrane (IMM). Electrons from NADH-linked and $FADH_2$-linked substrates enter at Complex I and II respectgively and are transferred to the final electron acceptor oxygen (O_2) that is fully reduced to water. As electrons flow down the respiratory chain, protons are pumped into the intramembranous space that produces a proton motive force (dashed lines) that is used to drive ATP synthesis from ADP and Pi as protons move through the ATP synthase (Complex V). Flux analysis detects hydrogen ions produced by glycolytic activity of cells and oxygen consumption associated with mitochondrial oxidative phosphorylation (OXPHOS). Mitochondrial inefficiencies include proton leak and electron leak. Protons may move back into the mitochondrial matrix at sites other than the ATP synthase in process known as proton leak that dissipates the proton motive force without concomitant synthesis of ATP. Leakage of electrons from the respiratory chain result in the formation of superoxide ($O_2^{-\cdot}$) and several other reactive oxygen species (ROS). Oxidation of lipids by ROS can lead to lipid peroxidation and formation of a secondary lipid peroxide, 4-hydroxy 2-nonenal (4-HNE). 4-HNE has been shown to increase proton leak via increased activity of uncoupling proteins (UCP's).(Adapted from Bottje and Carstens, 2012).

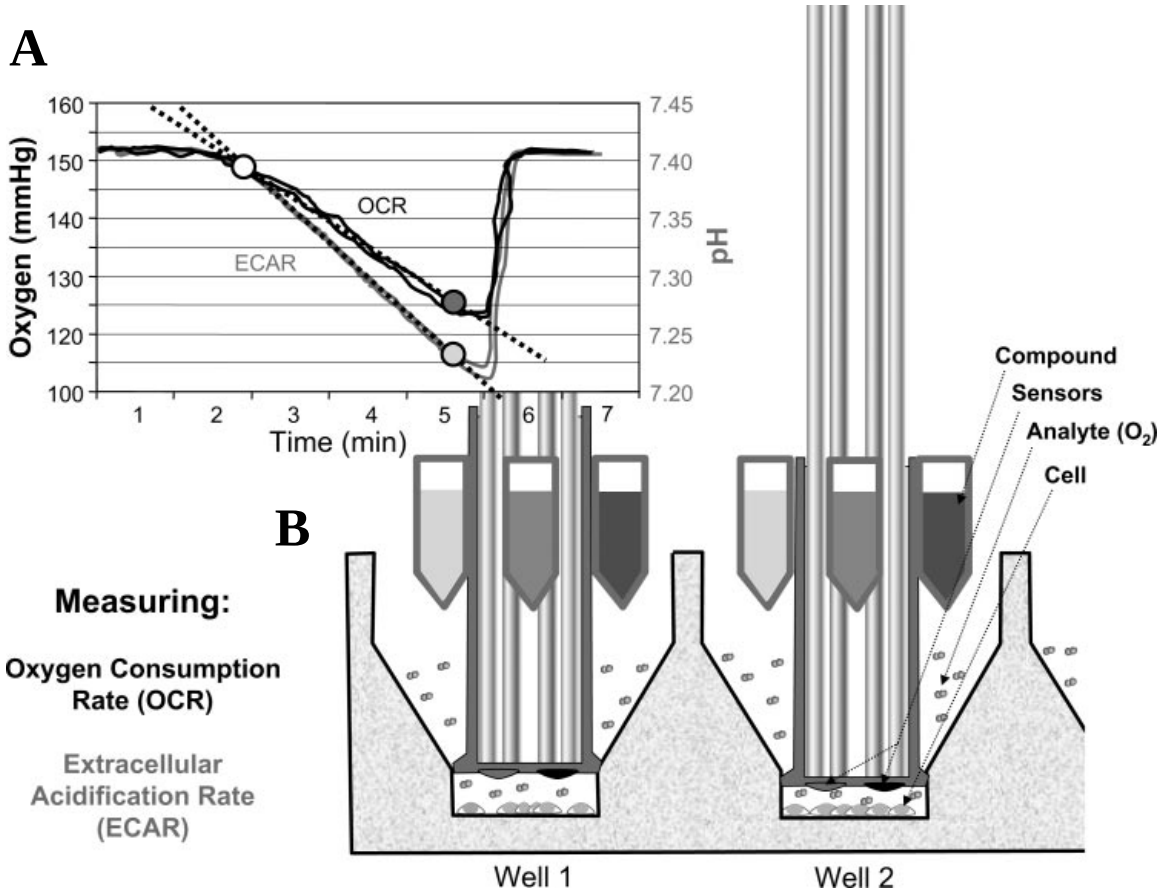

Figure 2.2: Depiction of A.) Determination of oxygen consumption rate (OCR) and extracellular acidification rate (ECAR) based on slopes of changes in oxygen and pH in the media B.) Probes containing light guides that detect levels of oxygen and hydrogen ion in the media surrounding a monolayer of cells in each well (see text for details) (Reproduced with permission from Seahorse Biosciences, Billerica MA, from Wu et al., (2007)

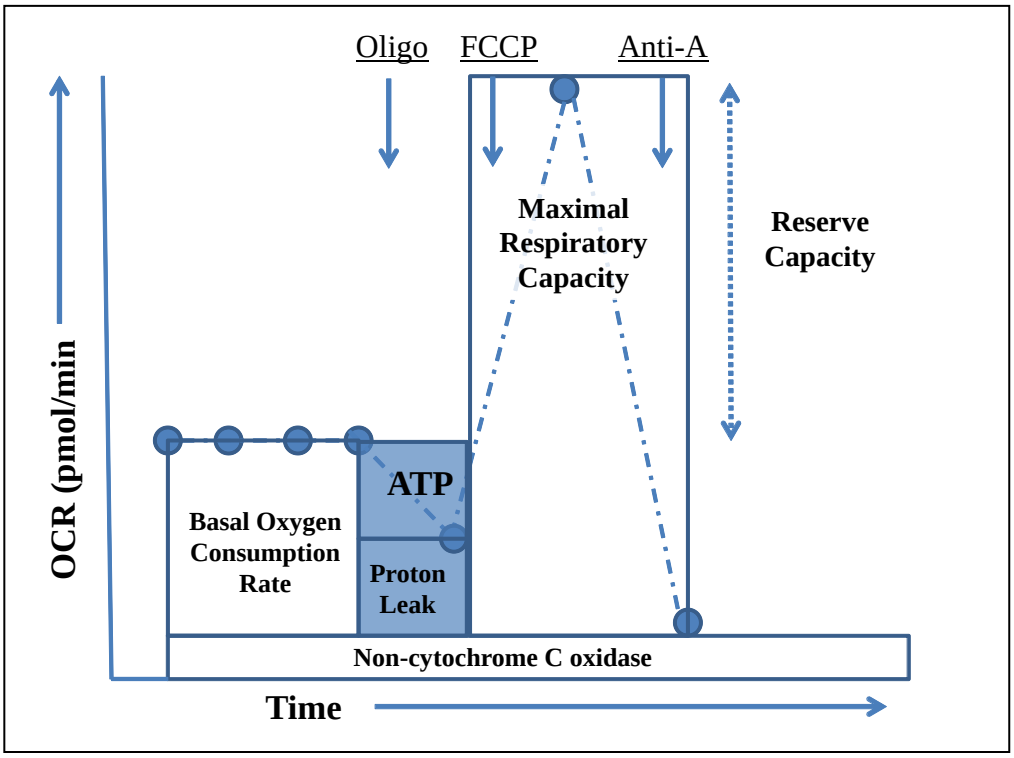

Figure 2.3: Measurement of indices of mitochondrial function using 'BOFA' analysis that is derived by measuring oxygen consumption rate (OCR) during basal conditions [B], that is followed by treatment of cells with oligomycin [O], FCCP [F], and Antimycin A [A]) (From Hill et al., 2009). The decrease in OCR following oligomycin is attributed to ATP synthesis from ATP synthase activity. The treatment of cells or mitochondria with FCCP results in a maximal respiratory capacity of the cells. By subtracting basal OCR from maximal OCR, the reserve capacity of cells can be determined. Antimycin A (a Complex III inhibitor) blocks respiratory chain activity. By subtracting antimycin A inhibited OCR from oligomycin-inhibited OCR, the amount of oxygen consumed by proton leak in the cells can be determined. The remaining OCR following treatment of cells reveals non-cytochrome C oxidase-linked OCR which is comprised primarily of non-mitochondrial oxygen consumption (e.g. cellular activities of NADPH oxidase) as well as other oxygen consuming reactions such as the formation of reactive oxygen species from leakage of electrons from the electron transport chain.

A

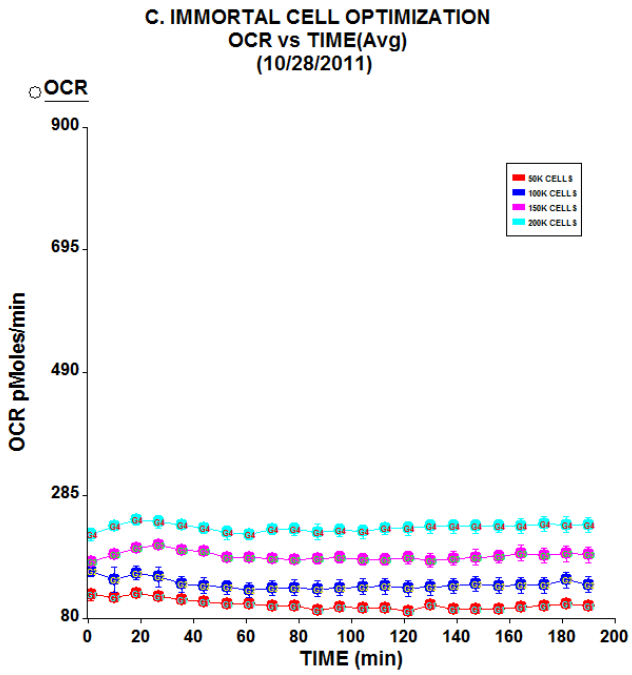

B

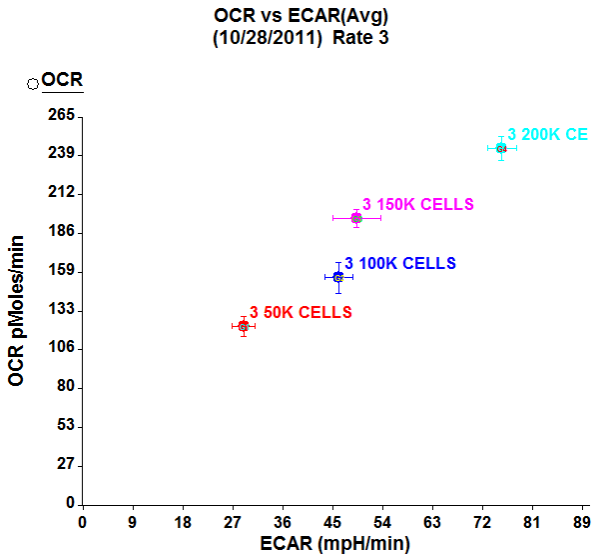

Figure 2.4: A) Effects of cell seeding density (number of cells added per well from 50,000 to 200,000 [K]) in Chicken Embryonic Liver Immortalized (CELi-im) cells on A) oxygen consumption rate (OCR, pmoles per min) over a 180 min period, and B) OCR and extracellular acidification rate (ECAR) at time point 3. The values represent the mean ± SE of 3 to 4 observations per seeding density**. B)** Relationships of OCR and ECAR for the different cell densities obtained at the third measurement.

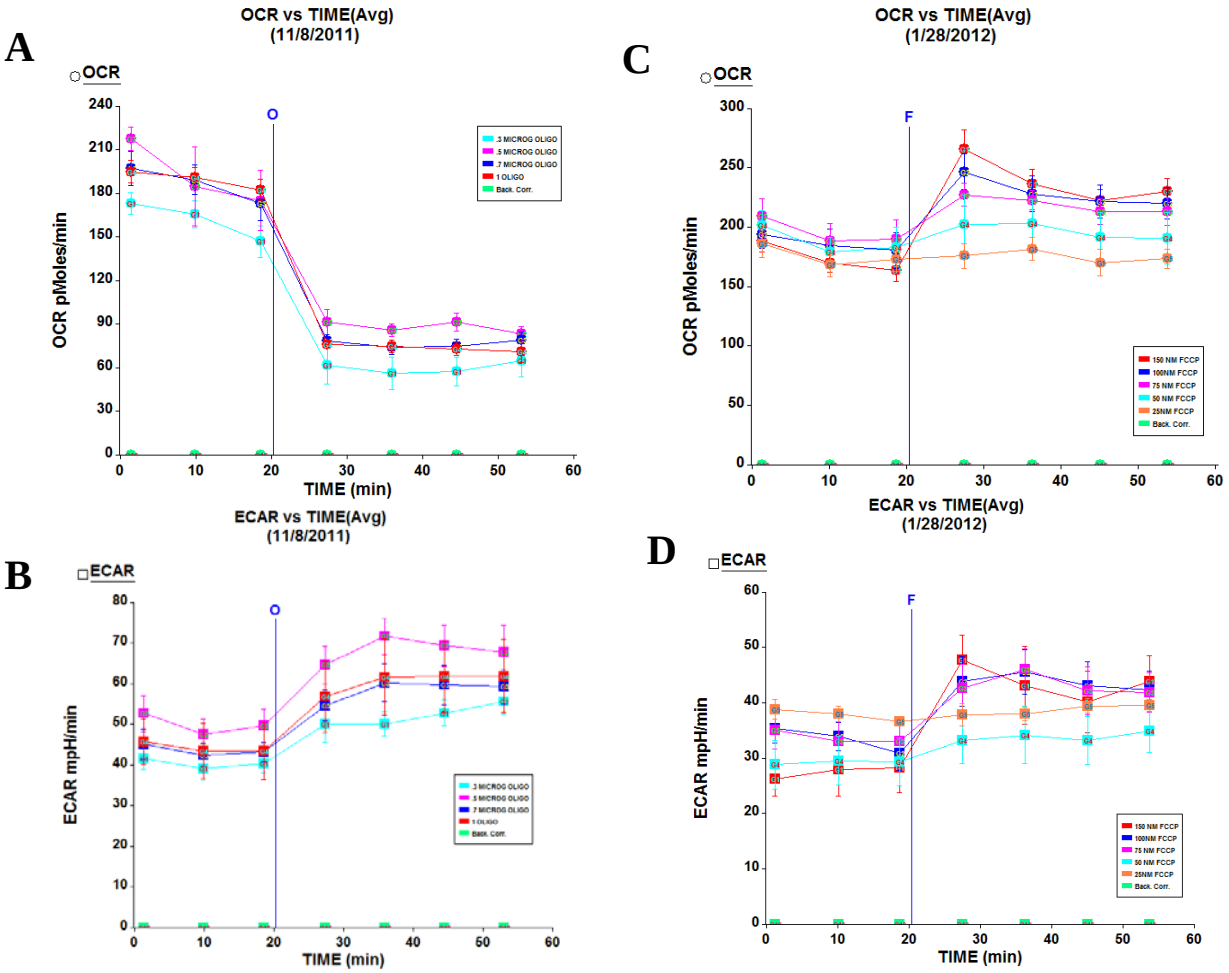

Chicken embryonic liver-immortalized (CELi-im) cells

Figure 2.5: Effects of oligomycin (0.3 to 0.1 µg/mL final concentration) and Carbonyl cyanide-p-trifluoromethoxyphenylhydrazone, FCCP (25 to 150 nM final concentration) on oxygen consumption rate (OCR, pmoles/min) (A, B) and extracellular acidification rate (ECAR) (C, D) in Chicken Embryonic Liver immortalized cells (CELi-im). Values represent the mean ± SE of 3 to 4 observations in oligomycin and 4 to 5 in FCCP.

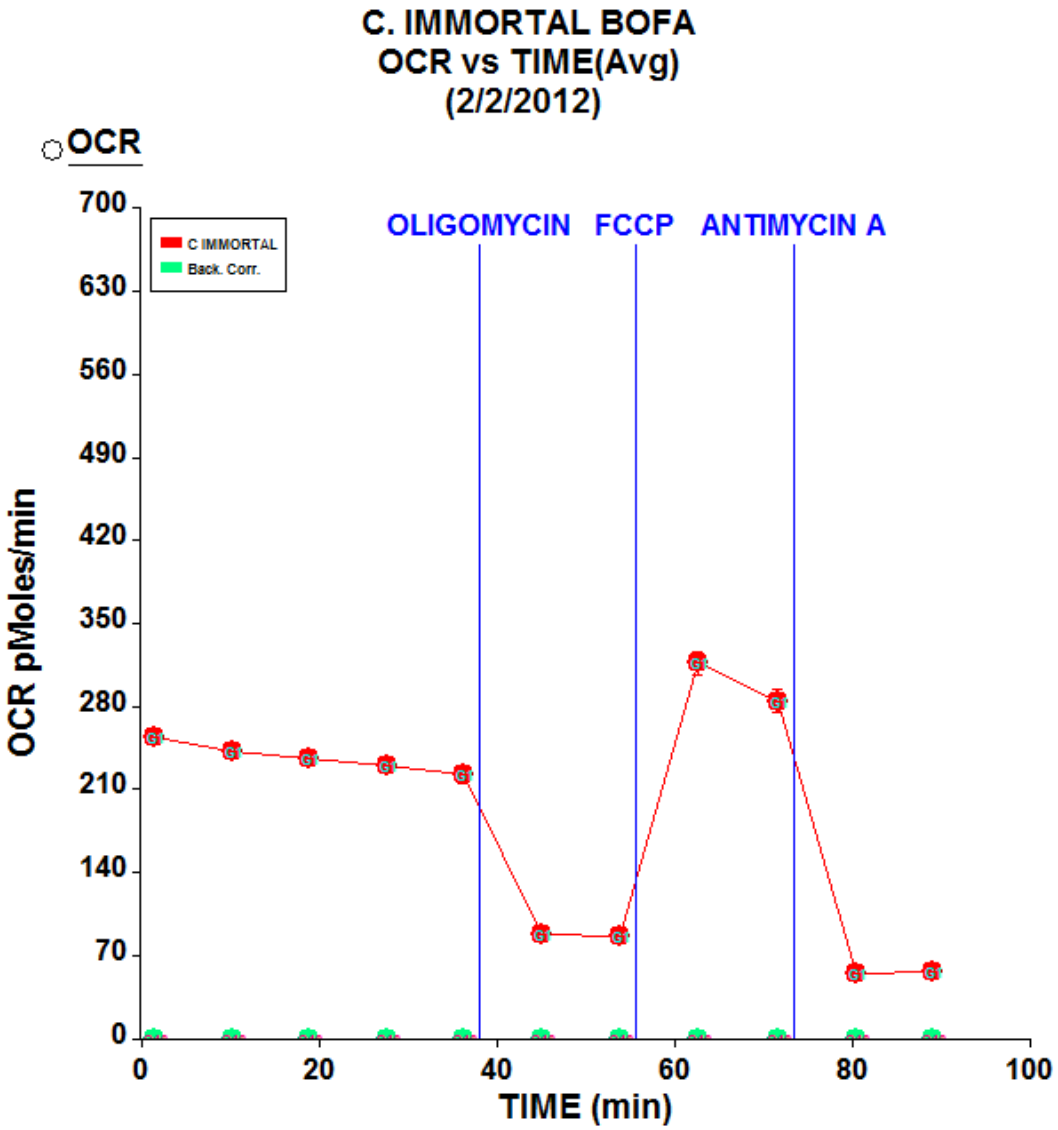

Figure 2.6: Bioenergetic analysis ('BOFA' analysis) of Chicken Embryonic Liver Immortalized (CELi-im) cells using the sequential measurements of oxygen consumption rate (OCR) during a Basal period followed by addition of Oligomycin (1 □g/mL), Carbonyl cyanide-p-trifluoromethoxyphenylhydrazone, FCCP (150 nM) and antimycin A (10 μM). The values represent the mean ± SE of 20 observations. The graph inset represents oxygen consumption of CELi cells associated with reserve capacity, ATP synthesis, proton leak and non-mitochondrial (Mito) mechanisms. (See Figure 1.3).

A

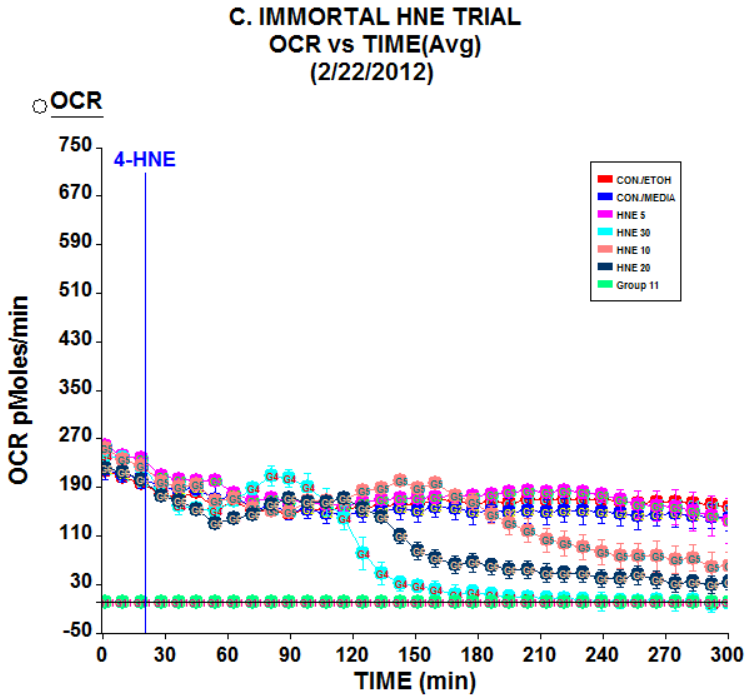

B

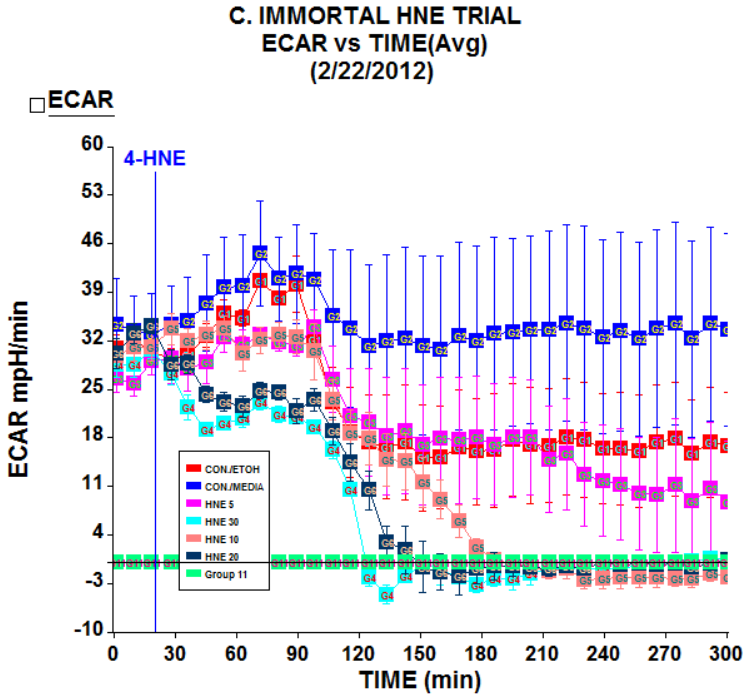

Figure 2.7: Effects of 4-hydroxy 2-nonenal (4-HNE) (5 to 30 μM final concentration) on oxygen consumption rate (OCR) in chicken embryo liver immortalized (CELi-im) cells (100,000 cells/well). Values represent the mean ± SE of 3 to 5 observations.

A

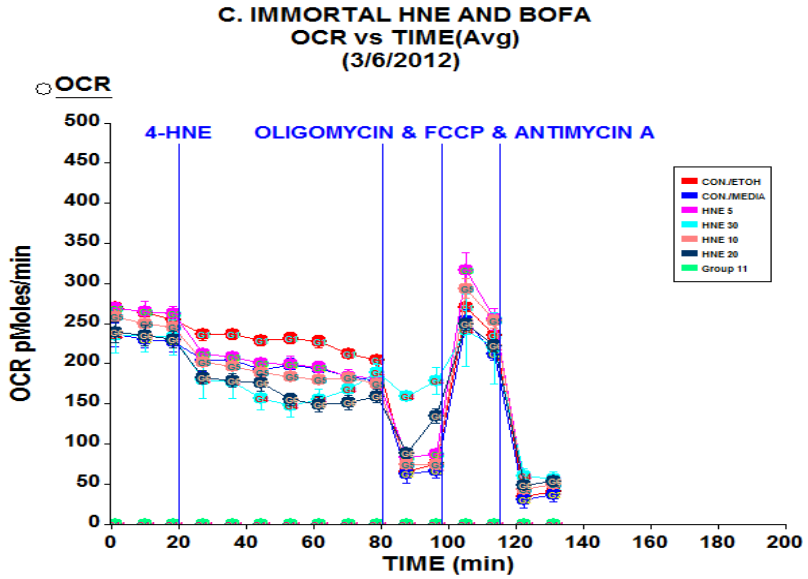

B

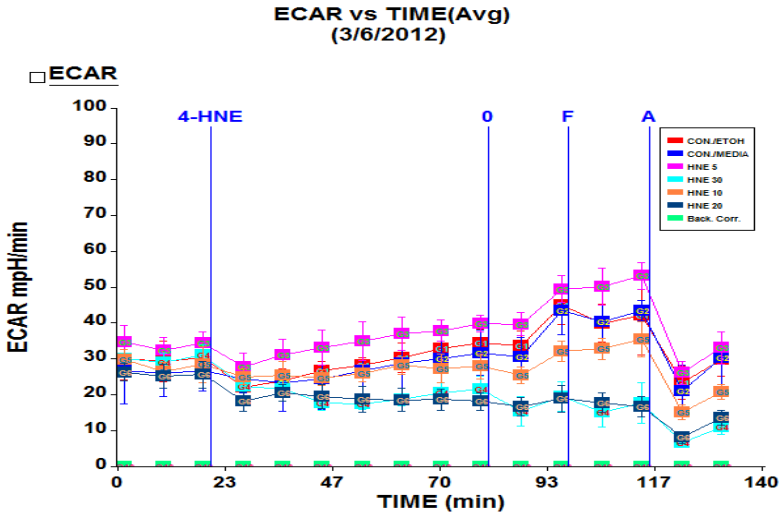

Figure 2.8: The effect of 4-hydroxy 2-nonenal, 4-HNE (5 to 30 µM final concentration) and sequential treatments of oligomycin (1 µg/mL), Carbonyl cyanide-p-trifluoromethoxy-phenylhydrazone, FCCP (200 nM), antimycin A (10 µM) on A) oxygen consumption rate (OCR) and B) Extracellular acidification rate (ECAR, mpH/min) in Chicken Embryonic Liver Immortalized (CELi-im) cells.
Values represent the mean ± SE of 3 to 5 observations.

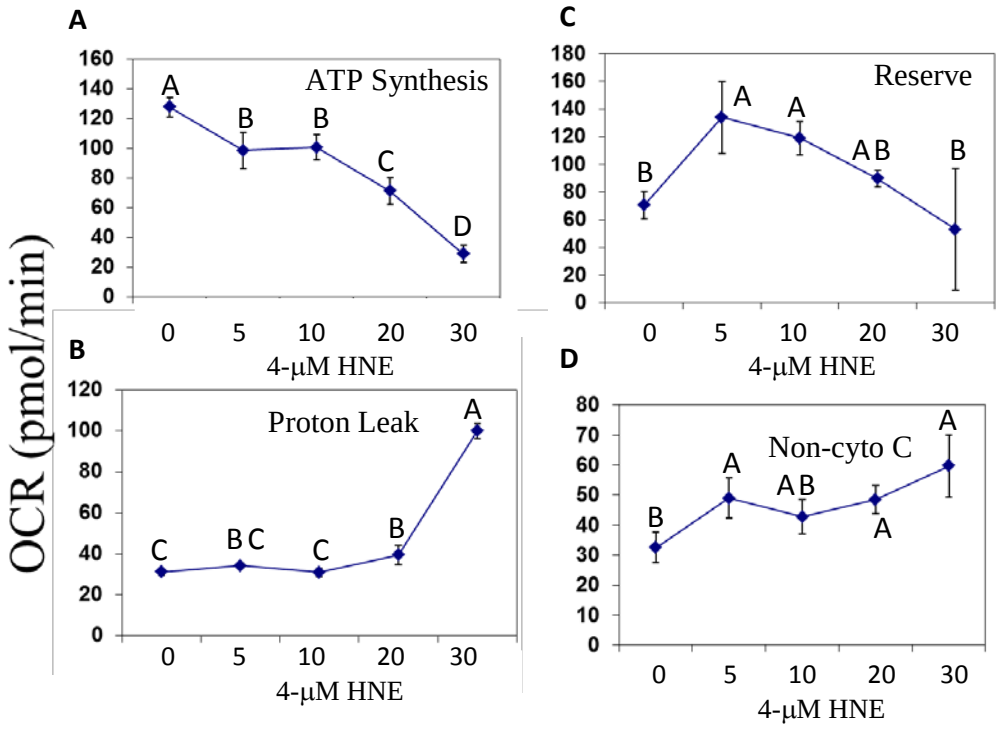

Figure 2.9: Effects of 4-hydroxy nonenal (4-HNE, 0 to 30 μM) on oxygen consumption rates (OCR, pmol/mL) associated with ATP synthesis, reserve capacity, proton leak and non-cytochrome c oxidase activities in chicken embryo liver immortal (CELi-im) cells. Each component was determined from data that is presented in Figure 2.9 using equations shown in Table 2.1.
Each value represents the mean ± SE of 3 to 5 observations.

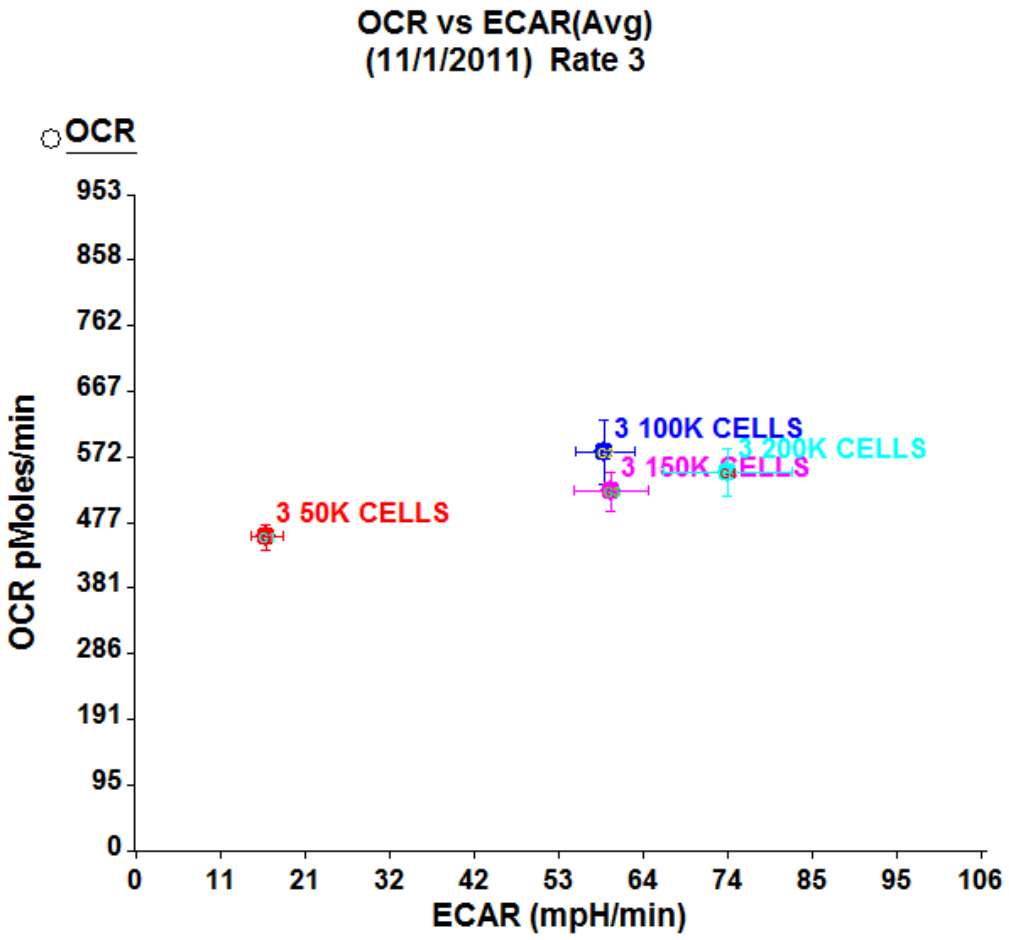

Figure 2.10. Oxygen consumption rate (OCR, pmol/min) and extracellular acidification rate (mpH/min) ECAR relationships in Leghorn Male Hepatoma (LMH) hepatocytes with seeding rates of 50,000 (50K), 100K, 150K and 200K per well. The relationship is shown after the third (3) measurement.
Values represent the mean $\pm$ SE of 3 to 5 observations per seeding density

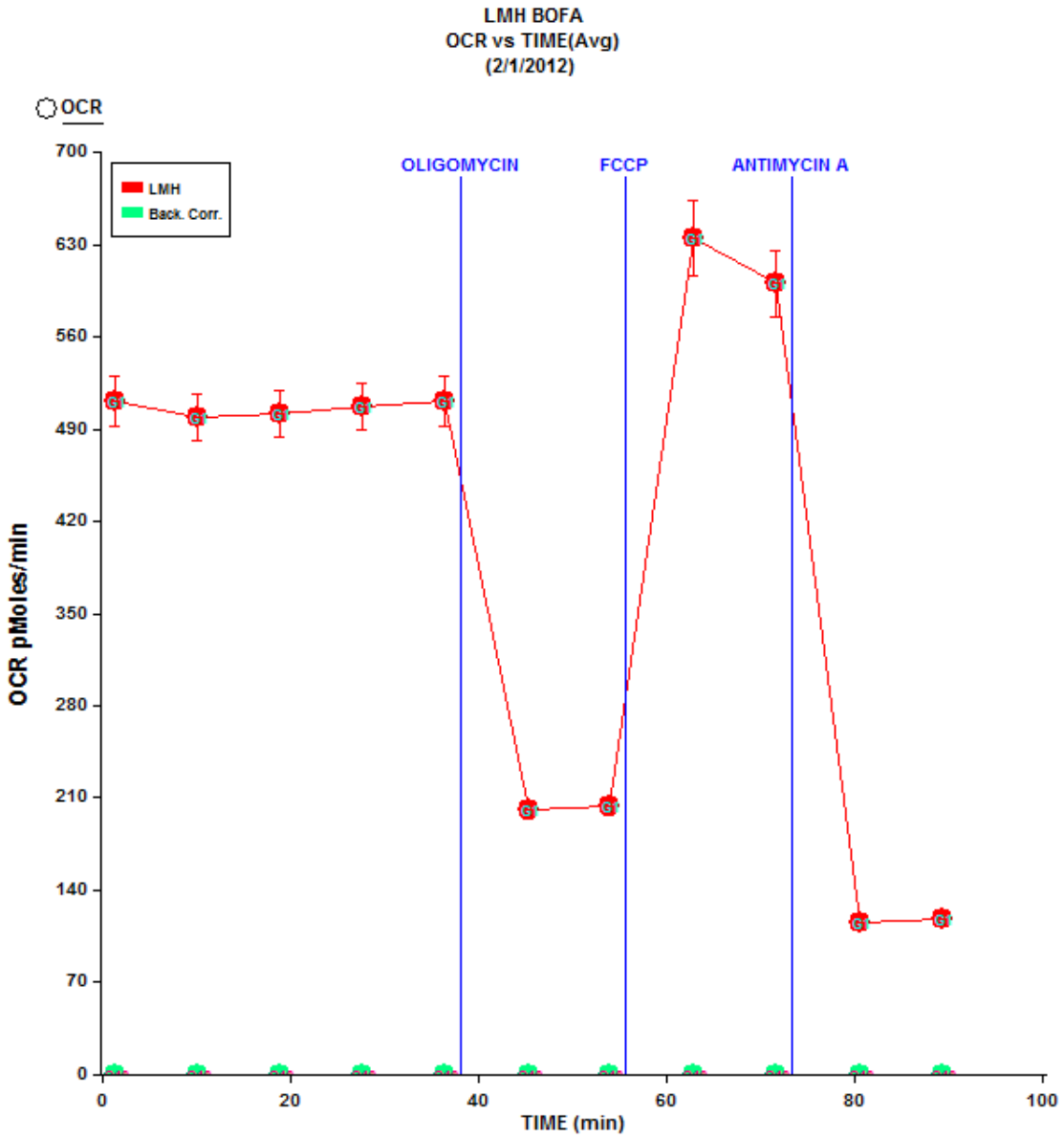

Figure 2.11: Bioenergetic analysis ('BOFA' analysis) of Leghorn Male Hepatoma (LMH) cells using the sequential measurements of oxygen consumption rate (OCR) during a Basal period followed by addition of oligomycin (1 µg/mL), Carbonyl cyanide-p-trifluoromethoxy-phenylhydrazone, FCCP (150 nM) and antimycin A (10 µM). The values represent the mean ± SE of 20 observations. The graph inset represents oxygen consumption of LMH cells associated with reserve capacity, ATP synthesis, proton leak and non-mitochondrial (Mito) mechanisms. (See Figure 1.3).

A

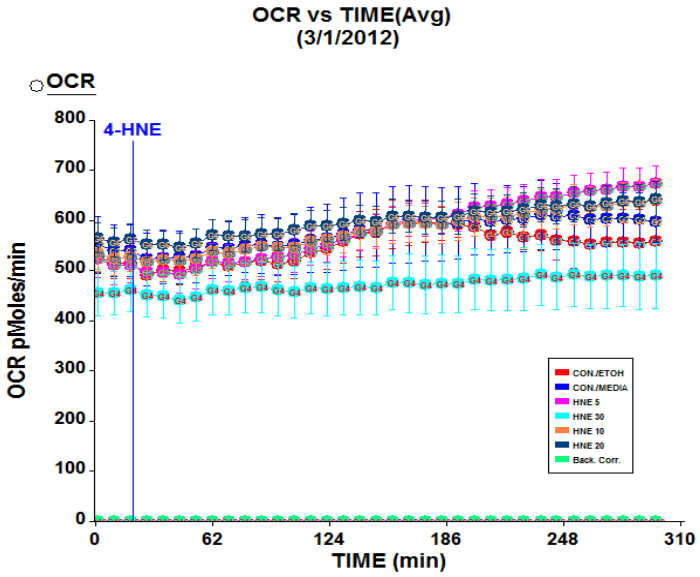

B

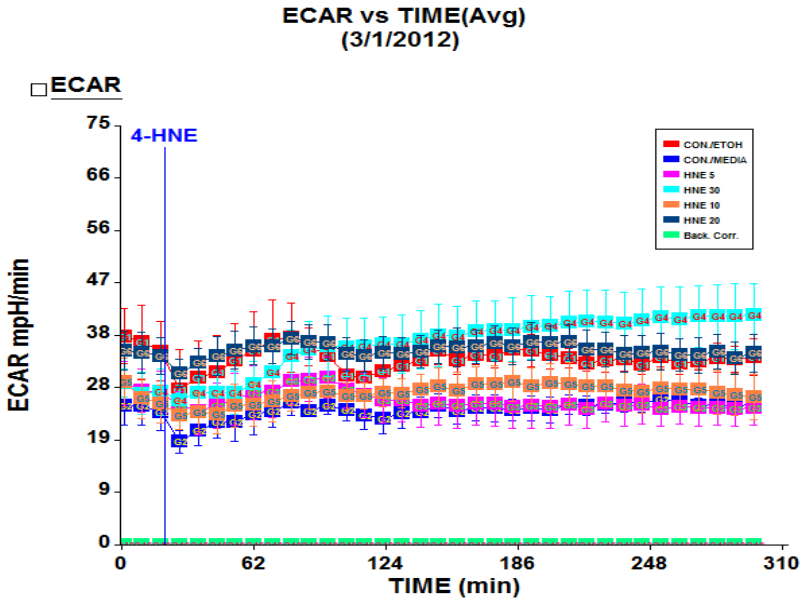

Figure 2.12: Effects of 4-hydroxy 2-nonenal (4-HNE) (5 to 30 μM final concentration)on A) oxygen consumption rate (OCR, pmol/min) and B) extracellular acidification rate (ECAR, mpH/min) in Leghorn Male Hepatoma (LMH) cells (50,000 cells/well).
Values represent the mean ± SE of 3 to 5 observations.

A

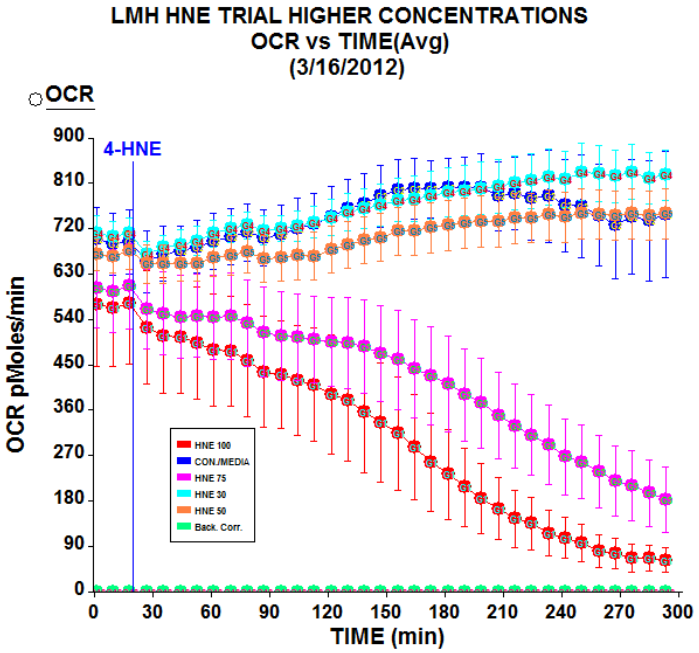

B

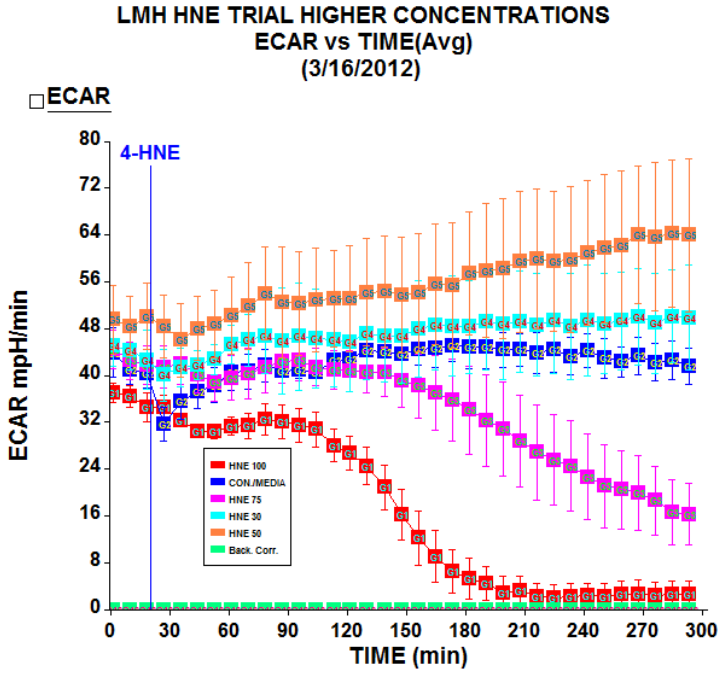

Figure 2.13: Effects of 4-hydroxy 2-nonenal (4-HNE) (0 to 100 μM final concentration) on A) oxygen consumption rate (OCR, pmol/min) and B) extracellular acidification rate (ECAR, mpH/min) in Leghorn Male Hepatoma (LMH) cells (50,000 cells/well).
Values represent the mean ± SE of 3 to 5 observations.

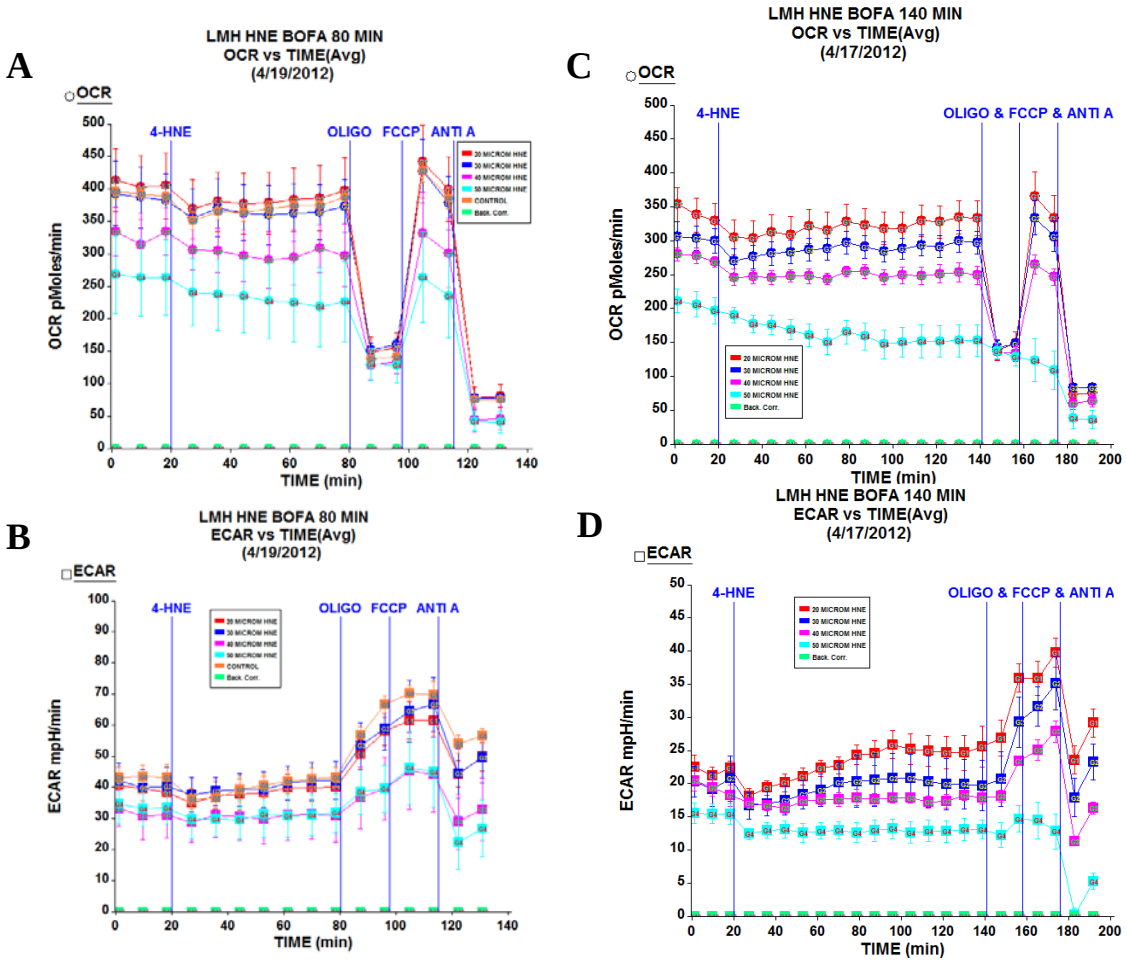

Figure 2.14: Bioenergetic assessment of effect of 4-HNE in leghorn male hepatoma (LMH) cells. After 3 measurements of basal oxygen consumption rate (OCR, pmol/min) and extracellular acidification rate (ECAR, mpH/min), cells were treated with 4-HNE (0, 20, 30, 40, or 50 μM) At 80 min and 140 min, LMH cells were treated with oligomycin (oligo, 1 μg/mL), carbonyl cyanide-p-trifluoromethoxyphenylhydrazone, (FCCP, 200 nM), antimycin A (10 μM) on oxygen consumption rate (OCR) in Leghorn Male Hepatoma (LMH) cells at 80 min oligomycin injection and 140 min oligomycin injection (A, B respectively). Values represent the mean $\pm$ SE of 3 to 5 observations.

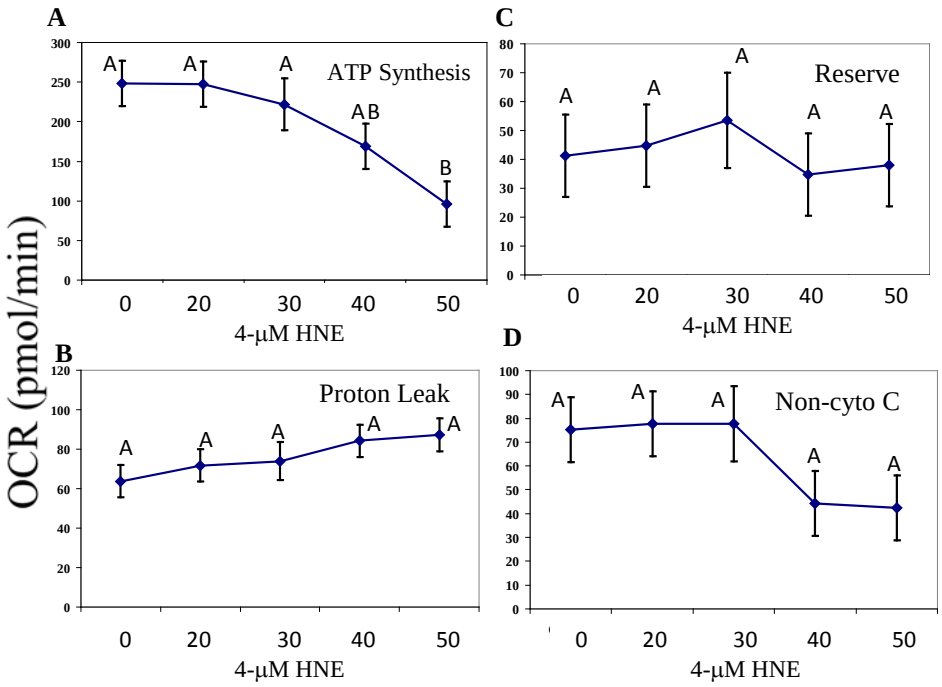

Figure 2.15: Effects of 4-hydroxy nonenal (4-HNE, 0 to 50 μM) on oxygen consumption rates (OCR, pmol/mL) associated with ATP synthesis, reserve capacity, proton leak and non-cytochrome c oxidase (Non-cyto C) activities in leghorn male (LMH) cells. Each component was determined from data that is presented in Figure 2.16 A (initiated at 80 min following 4-HNE treatment) using equations in Table 2.1.
Each value represents the mean ± SE of 3 to 5 observations.

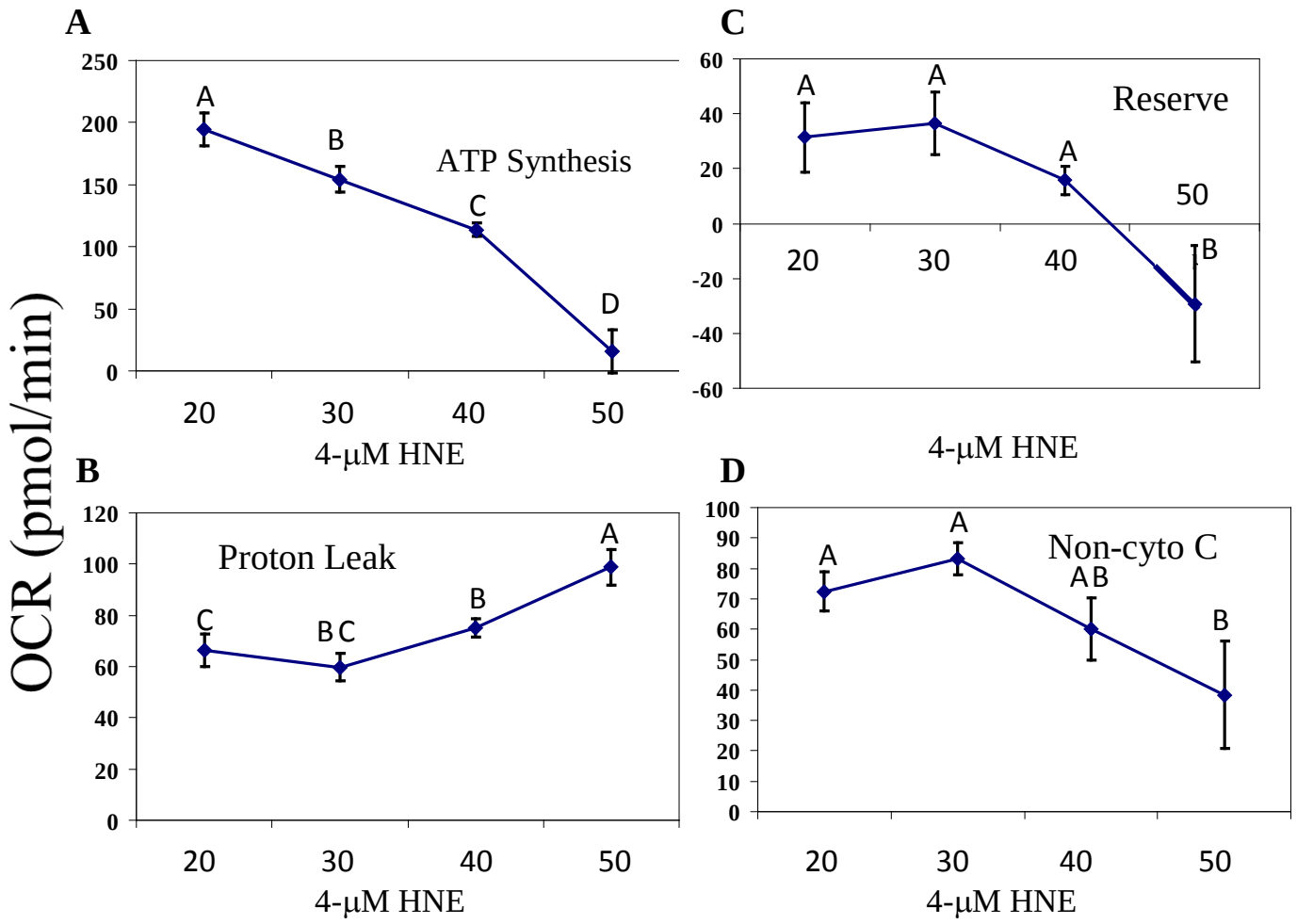

Figure 2.16: Effects of 4-hydroxy nonenal (4-HNE, 0 to 50 μM) on oxygen consumption rates (OCR, pmol/mL) associated with ATP synthesis, reserve capacity, proton leak and non-cytochrome c oxidase activities in leghorn male (LMH) cells. Each component was determined from data that is presented in Figure 2.16 C (initiated at 140 min following 4-HNE treatment) using equations Table 2.1
Each value represents the mean ± SE of 3 to 5 observations.

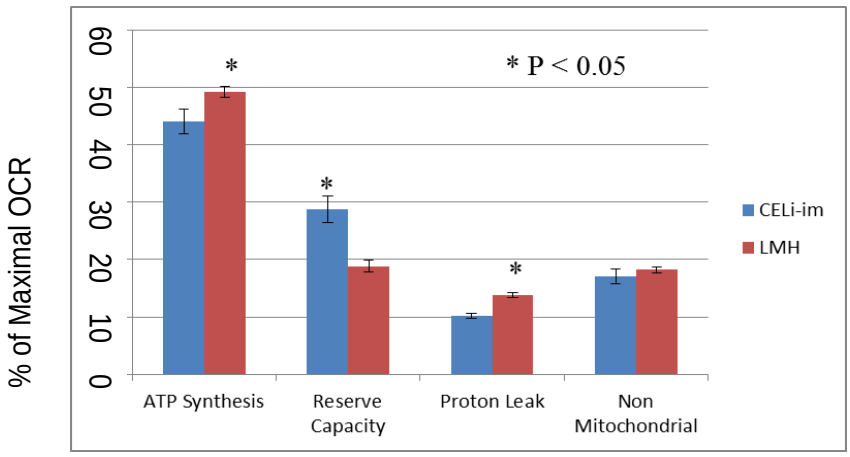

Figure 2.17. Comparison of mitochondrial bioenergetics expressed as a percent of maximum respriratory capacity in immortalized chicken embryo liver (CELi-im) and leghorn male hepatoma (LMH) hepatocyte lines under basal conditions. The bars represent the means $\pm$ SE (n=20) that were calculated from data presented in Figures 2.6 and 2.12 for CELi-im and LMH cells, respectively

*Mean values are higher ($P < 0.05$)

APPENDICES

APPENDIX I

Assessment of bioenergetics in intestinal tissue from neonatal broiler chicks[1]

Piekarski A., K. Lassiter, K. Byrne, B.M. Hargis, and W.G. Bottje. 2011

Abstract: Poult. Sci. 90(1):179

[1]Material that is provided in this chapter was presented in a poster at the 104th Annual meeting of the Poultry Science Association in St. Louis, MO, July17 – 20, 2011.

ABSTRACT

The primary objective of this study was to develop methodology for assessing intestinal bioenergetics (aerobic respiration and glycolysis) by flux analysis of oxygen consumption rate (OCR) and extracellular acidification rate (ECAR) that reflect mitochondrial and glycolytic activities, respectively. Using sequential additions of oligomycin (inhibitor of ATP synthase, FCCP (uncoupler of oxidative phosphorylation), and Antimycin-A (electron transport chain inhibitor), oxygen consumption linked to ATP synthesis and proton leak, maximal oxygen consumption and oxygen reserve capacity of cells, as well as oxygen consumption linked to activities of oxidases and mitochondrial reactive oxygen species production can be determined. The XF24 Flux analyzer (Seahorse Biosciences, Billerica MA) used in these studies creates a 7 μl chamber in each well of a specially designed 24 well microtiter plate. In our approach, mid-jejunal tissue rings (~1-2 mm wide) were obtained from neonatal broiler chicks (< 48 h post hatch) using a scalpel for sectioning under a dissection microscope. The intestinal rings were placed in each well in growth media (DMEM with 10% fetal bovine serum and1% Pen-Strep) and covered with a screened islet to hold the tissue in place. The intestinal rings were washed with Seahorse analyzer media and incubated for 1 hour in a non-CO2 incubator while the analyzer probes were calibrated. Once probes were calibrated, the cells were placed into the machine for a runtime of up to 5 hours with OCR and ECAR measurements obtained at 5 to 10 min intervals. During this time energy substrates and/or chemicals can be introduced through the ports in the Seahorse Flux Pak cartridges to assess intestinal bioenergetics. The long term goal of these studies is to identify effects that a wide range of factors (e.g. dietary

components, microbial populations) have on intestinal bioenergetics that in turn play important roles in productivity and health in commercial poultry. The major objective of this study was to develop methodology to investigate intestinal bioenergetics using intact pieces of gut tissue (slices, rings of biopsies) in the gastrointestinal tract in 1 day old broilers.

INTRODUCTION

Gut health is extremely important in animal agriculture. The gut is a highly dynamic organ with its entire mucosal surface being shed and replaced with new cells every 3 to 5 days. The ability of the gut to respond to pathogens, to transport nutrients, and to generate a new complement of cells every 3 to 5 days requires vast energy expenditures. Thus, *bioenergetics*, the generation of ATP either by oxidative phosphorylation in the mitochondria or through glycolysis in the cytosol, *is absolutely critical in maintaining a healthy, functional gastrointestinal tract.*

Enterocytes are simple columnar epithelial cells found in the small intestine and colon. These cells play a secretory role as well as aid in the digestion and transport of molecules from the intestinal lumen. The preferred fuels of respiration for enterocytes are: glucose, glutamine, and glutamate (Watford et al., 1979). Further biochemical studies have confirmed that glutamine gained from the intestinal lumen or vasculature is the main substrate sustaining small intestinal epithelial cells (enterocytes) (Roediger et al., 1990). Using new techniques in studying bioenergetics, we can confirm these as well as compare them to the effects of probiotics on enterocytes.

MATERIALS AND METHODS

Animals – Tissues: Newly hatched broiler chicks from a commercial hatchery were humanely killed by cervical dislocation and the ileum removed. The ileum was flushed with cold buffer (DMEM). All procedures were carried out with wet ice and ice cold buffer. Ileal rings and slices (~1-2 mm) were obtained with a scalpel; biopsies were obtained using a biopsy needle (2 mm i.d.).

Oxygen consumption rate (OCR) and extracellular acidification rate (ECAR) were assessed with an XF24 Flux Analyzer (Seahorse Biosciences, North Billerica, MA) (See Methods, Flux Analysis; A). The Flux Analyzer measures OCR and ECAR in specialized microplates and cover plates (B) equipped with probes to monitor PO2 and pH (C). The rate of change of PO2 and pH is monitored and OCR and ECAR determined from the slope (D). During an experiment, chemicals can be added to each well through 4 different ports/well (E). Bioenergetics can be determined by sequential additions of Oligomycin, FCCP, and Antimycin A (e.g. Hill et al., 2009) (F). For all bioenergetic studies, the culture medium was changed to an unbuffered DMEM media containing 25 mM glucose 60 min prior to the initiation of OCR and ECAR measurements.

Methods – Flux Analysis:

1) Place intestinal tissue in culture plates prepared with Cell Tak; cover with 30 mL media for 45 min.
2) Add unbuffered media and place in non-CO2 incubator for 1 h.
3) Place plate and specialized cover plate in flux analyzer.
4) Detection of oxygen and H+:
    a) Excitation wavelengths of
    b) 532 and 470 nm l that
    c) Stimulates fluorophores for O2 and H+ and
    d) Emits fluorescent signal
    e) That is detected by photodetectors in flux analyzer

5) Calculation of oxygen Consumption Rate (OCR) and extracellular acidification rate (ECAR) from slope (flux) of PO2 and pH changes in each well; 4 wells have media only for background correction across a plate.

6) Four ports in the cover plate next to each waveguide of each well allow for pneumatic addition of chemicals (e.g. chemical inhibitors, substrates). The up and down movement of cover plate probes occurs to quickly mix media contents after chemicals are added to the wells.

7) Bioenergetics can be determined by monitoring OCR to sequential additions of oligomycin* (Oligo), FCCP**, and Antimycin-A*** (Anti-A). This enables the assessment of basal OCR, OCR linked to mitochondrial ATP production, OCR linked to proton leak, maximal respiratory capacity, O2 consumption reserve capacity, and non-mitochondrial OCR such as shown in the figure from Hill et al. (2009).

RESULTS

OCR:

Results indicate that cells/mitochondria were functional, responding appropriately to energy substrate (increased OCR to Glu-Pyr) and to electron transport chain inhibition (decreased PCR following addition of Antimycin A) (Figure 1 A). FCCP had no effect on OCR which might be due to thickness of tissue slice (Schuh et al., 2011) (Figure 1 A, p. 71).

ECAR:

The chemicals had little effect on ECAR, with the steep decline in OCR prior to first chemical treatment suggesting that the intestinal slice preparation may not have had time to completely stabilize (Figure 1 B, p 71).

There were no differences between intestinal slices or biopsies in response to chemical treatments (Figure 2, p. 72). As in previous studies, intestinal tissue appeared to respond to energy substrate and Antimycin A, but not to uncoupling with FCCP. Tissues also were not responsive to ATP synthase inhibition with Oligomycin.

OCR increased in response to media with little change following FCCP. OCR decreased in response to Oligomycin over a long period of time. Antimycin caused an abrupt decrease in OCR. Bovine serum albumin had no effect on responses of OCR to chemicals or energy substrate. It does appear that OCR measurements can be made over long time periods (Figure 3, p. 73).

Summary

In summary. it was determined that:

1) Intestinal tissue (rings, slices and biopsies) exhibited an increase in OCR to substrate (glucose-pyruvate) and a decrease following Antimycin-A (Complex III inhibitor), but were not responsive to uncoupling with FCCP or to ATP synthase inhibition with Oligomycin (short term, Fig. 2). Tissue did appear to be responsive long term to Oligomycin (Fig. 3). Possibly, the tissues used in these studies were too thick (too many cell layers) which was evident from the high level of OCR observed in this study compared to studies recently conducted with chicken embryo fibroblasts in our lab (K. Lassiter).
2) We suspect that difficulties in centering the tissues in the middle of the well caused considerable noise in OCR measurements (not shown)

3) We plan to develop methods for measuring bioenergetics in enterocytes in primary cell culture as an alternative approach to attempts shown here with intestinal rings, slices and biopsies shown in the present study.

References

Hill, B. et al. 2009. Importance of bioenergetic reserve capacity in response to cardiomyocyte stress induced by 4-hydroxynonenal. Biochem. J. 424:99-107.

Shuh et al. 2011. Adaptation of microplate-based respirometry for hippocampal slice and analysis of respiratory capacity. J. Neuroscience Res (on line).

Figures

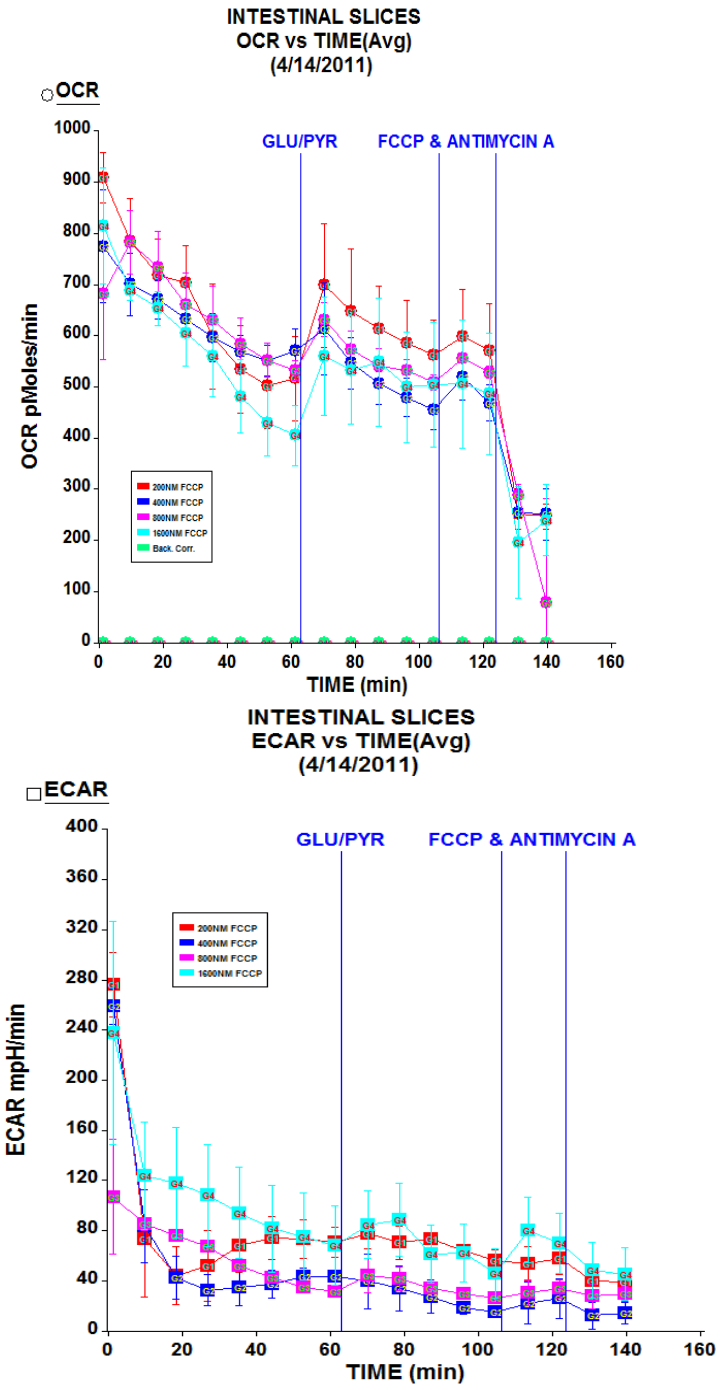

Fig. 1: OCR (1A) and ECAR (1B) response to energy substrate (Glu-Pyr), FCCP (uncoupler) and Antimycin A (Complex III inhibitor) in intestinal slices (~ 2 mm).

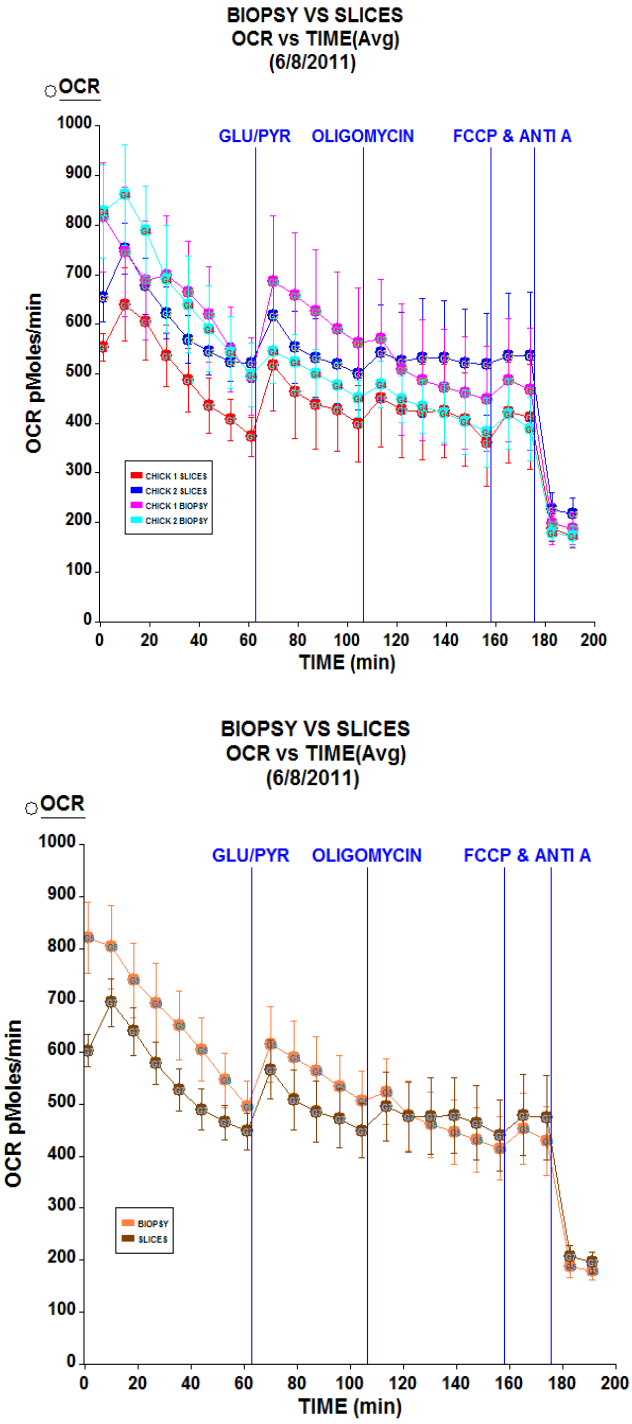

Fig. 2: OCR in intestinal biopsies (2 mm i.d.) and intestinal slices (1-2 mm) from two neonatal chicks (2A) in response to Glu-Pyr, Oligomycin, FCCP and Antimycin A. OCR values averaged for the two chicks for biopsies and slices are shown in 2B.

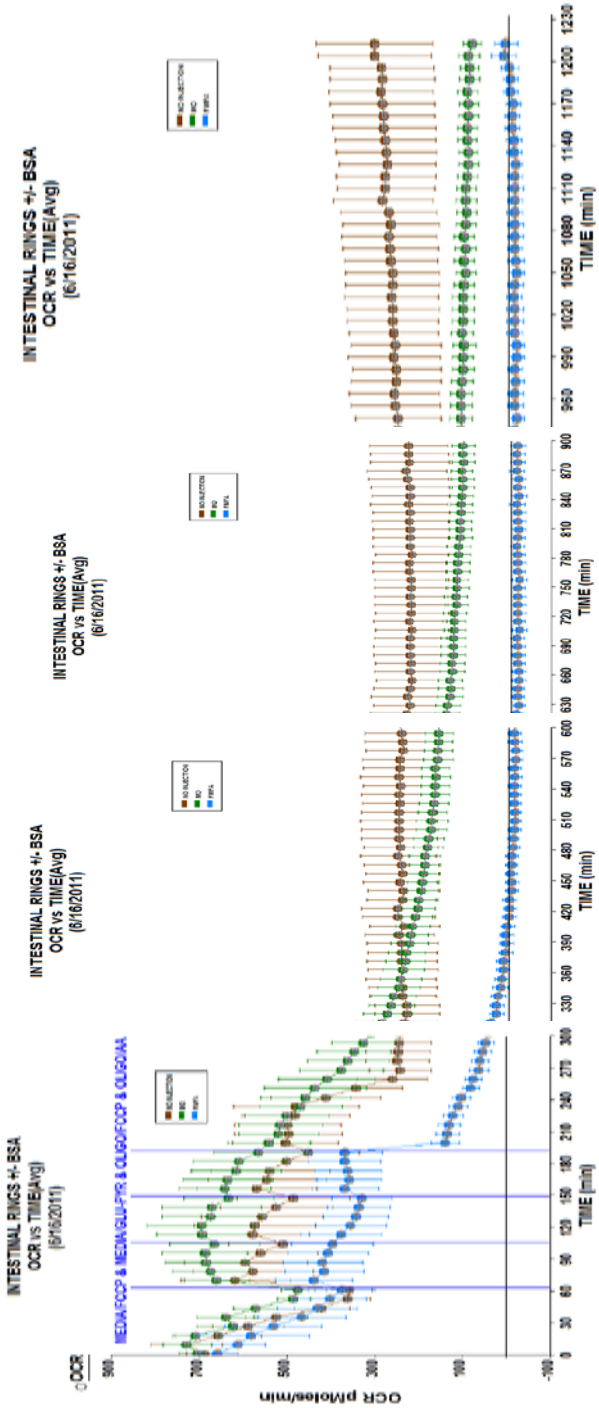

Fig. 3: OCR in intestinal rings over 20 h

Appendix II

Cell culture and Plating:

Cell lines used were LMH and CELi-im and were grown on polystyrene tissue culture dishes (BD Falcon).

1.) Cells of both lines were thawed out from liquid nitrogen by leaving vial inside hood for 15 min. Afterwards, cells were pipetted slowly to ensure even distribution and cells were plated onto polystyrene tissue culture plates for about 2 hours.

2.) After two hours plates were removed from the incubator and media was aspirated off and adherent cells were washed with PBS and fresh media was placed on top of the cells, (washing was to ensure removal of most DMSO from the old media).

3.) LMH cells required Waymouth's (Invitrogen-Gibco) media with 1% Penn-Strep, 1% Glutamine, and 10% FBS, whereas the CELi-im line required DMEM (Invitrogen-Gibco) with 1% Penn-Strep, 1% Glutamine, and 10% FBS.

4.) After media is prepared, cells are plated according to growth time and confluence. LMH seemed to grow faster than CELi-im, so LMH were plated by using 500 µl of cells in 9.5 mL of growth media and CELi-im were plated using 1 mL of cells and 9 mL of growth media.

Preparation of Chemicals to be Pneumatically injected:

Chemicals used in this experiment (Oligomycin, FCCP, Antimycin A, and 4-HNE) all started from a stock concentration and were diluted with DMSO to desired working concentrations before adding them to the assay media for placement in injection ports.

1.) Oligomycin was diluted with DMSO from a stock concentration of 50 mM to a working concentration of 1 mM; FCCP was diluted in DMSO from stock solution of 30 mM to a working concentration of 300 μM; and antimycin A was diluted with DMSO to a working concentration of 1 mM. 4-HNE was diluted using ethanol form a stock concentration of 64 mM to the needed concentration for the experiment.

2.) Chemicals were frozen at -20°C and thawed out the day of experiment. Chemicals were then mixed with assay media according to pre-calculated concentrations, and were then placed into the injection ports of the sensor plate.

3.) .) The concentrations of chemicals used were as follows: 1μg/mL Oligomycin, 200 nM FCCP, 10 μM Antimycin A, and multiple levels of HNE for the two cell lines (5, 10, 20, 30 μM CELi-im and 20, 30, 40, 50 μM LMH).

4.) Volumes for each port differ with port A holding 75 μl, B holding 83 μl, C holding 92 μl, and D holding 102 μl of chemical.

Pyruvate Additions:

Pyruvate was added to the assay media to provide the cells with an additional energy source.

1.) 30 mM Pyruvate was added to the assay media before the final volume of 575 µl was added to each well.

2.) This additional substrate was added straight into media instead of injection to ensure proper delivery to cells

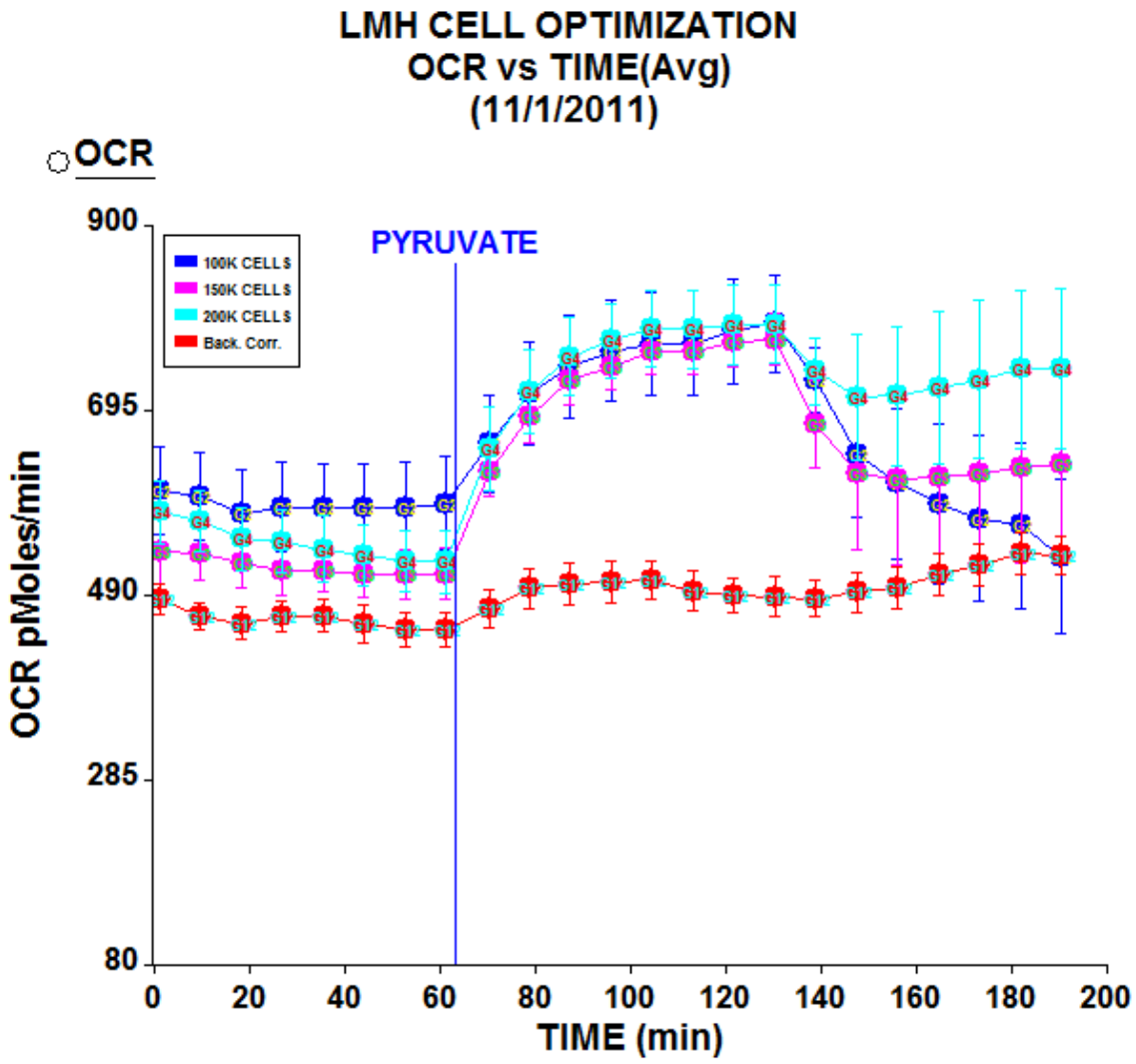

Preparation and Execution of Seahorse XF Analyzer

All experiments performed using a Seahorse XF Analyzer

1.) Day 0 cell lines are checked for confluence and then prepared for plating

2.) To prepare for plating cells are washed with PBS to wash away dead cells and 500 µl of 0.25% Trypsin is added and cells are placed in a 37°C, 5% CO_2 incubator, for 3 min to allow release of cells from the plate.

3.) Next, 5 mL of growth media was added to deactivate the effect of trypsin and cells centrifuged at 1000 rpm for 5 min in 14 mL polystyrene tubes (BD Falcon Biosciences) to form a pellet.

4.) The pellet is then resuspended in a small amount of growth media (1-2 mL) and 200 µl of these cells are mixed with 800 µl of Trypan blue for counting and percent alive calculated.

5.) Once the desired number of cells per well is calculated, plating begins with 100 µl per well, taking care not to add cells to the four background correction wells. An additional 150 µl of growth media is added after an hour of incubation to ensure survival overnight.

6.) A calibration plate is prepared by adding XF calibrant solution to each well of the sensor plate and then left in a 37°C non-CO_2 incubator overnight for hydration of probes.

7.) After plating, cells are kept in a 37°C, 5% CO_2 incubator overnight for growth

8.) The next morning, cells are washed with 1 mL unbuffered XF assay media and after washing, 575 µl of assay media is added as final volume before addition of chemicals during experiment.

9.) Cells are placed in a 37°C non-CO_2 incubator for 1 hr while any chemicals to be injected are prepared (see chemical preparation).

10.) Once chemicals are added to the injection ports of the sensor plate, the sensor plate is placed inside the machine for calibration.

11.) Finally, when the calibration is finished, the cell plate is placed in the XF Analyzer and the experiment is run for the desired amount of time according to the created protocol.